

Full-Duplex Cell-Free mMIMO Systems: Analysis and Decentralized Optimization

Soumyadeep Datta, Ekant Sharma, D.N. Amudala, Rohit Budhiraja and Shivendra S. Panwar, *Fellow*, IEEE

Abstract

Cell-free (CF) massive multiple-input-multiple-output (mMIMO) deployments are usually investigated with half-duplex (HD) nodes and high-capacity fronthaul links. To leverage the possible gains in throughput and energy efficiency (EE) of full-duplex (FD) communications, we consider a FD CF mMIMO system with *practical limited-capacity fronthaul links*. We derive closed-form spectral efficiency (SE) lower bounds for this system with maximum-ratio transmission/maximum-ratio combining (MRT/MRC) processing and optimal uniform quantization. We then optimize the weighted sum EE (WSEE) via downlink and uplink power control by using a two-layered approach: the first layer formulates the optimization as a generalized convex program (GCP), while the second layer solves the optimization decentrally using alternating direction method of multipliers. We analytically show that the proposed two-layered formulation yields a Karush-Kuhn-Tucker point of the original WSEE optimization. We numerically show the influence of weights on the individual EE of the users, which demonstrates the utility of WSEE metric to incorporate heterogeneous EE requirements of users. We also show that with low fronthaul capacity, the system requires a higher number of fronthaul quantization bits to achieve high SE and WSEE. For high fronthaul capacity, higher number of bits, however, achieves high SE and a reduced WSEE.

Index Terms

Decentralized optimization, energy efficiency, full-duplex (FD), limited-capacity fronthaul.

I. INTRODUCTION

Massive multiple-input-multiple-output (mMIMO) wireless systems employ a large number of antennas at the base-stations (BSs), and achieve higher spectral efficiency (SE) and energy efficiency (EE) with relatively simple signal processing [1]–[3]. Two distinct mMIMO variants are being investigated in the literature: i) co-located, wherein all antennas are located at one place [1]; and ii) distributed, wherein antennas are spread over a large area [2], [3]. While co-located mMIMO systems have a low fronthaul requirement, distributed mMIMO systems, at the

Soumyadeep Datta, Ekant Sharma, Dheeraj Naidu Amudala and Rohit Budhiraja are with the Department of Electrical Engineering, IIT Kanpur 208016, India. email: {sdatta, ekant, dheeraja, rohitbr}@iitk.ac.in. Soumyadeep Datta and Shivendra S. Panwar are with the Department of Electrical and Computer Engineering, NYU Tandon School of Engineering, Brooklyn, NY 11201, USA. email: {sd3927, sp1832}@nyu.edu. A part of this work is submitted for peer review in IEEE International Conference on Communications (ICC) 2021.

cost of higher fronthaul infrastructure, have greater spatial diversity to exploit and consequently have greater immunity to shadow fading [2]. Cell-free (CF) mMIMO is one of the most promising distributed mMIMO variants in the current literature [2], [3]. CF mMIMO envisions a communication region with no cell boundaries, where all access points (APs) communicate with all UEs. CF mMIMO promises substantial gains in SE and fairness over small-cell deployments [2], [3].

Full-duplex (FD) wireless communication has recently been practically realized with advanced self-interference (SI) cancellation mechanisms [4]. FD CF mMIMO is a relatively recent area of interest [5]–[7], where APs simultaneously serve downlink and uplink UEs on the same spectral resource. Vu *et al.* in [5] considered a FD CF mMIMO system with maximum-ratio combining and showed that if SI at the APs is suppressed up to a certain limit, it has higher throughput than a FD co-located and half-duplex (HD) CF mMIMO systems. Wang *et al.* in [6] evaluated the sum rate of a network-assisted FD CF mMIMO system using zero-forcing (ZF) and regularized zero-forcing (RZF) beamforming. Nguyen *et al.* in [7] proposed a novel heap-based algorithm for pilot assignment to overcome pilot contamination in FD CF mMIMO systems.

In CF mMIMO, APs are connected to a central processing unit (CPU) using fronthaul links. The existing FD CF mMIMO literature assumes high-capacity fronthaul links [5]–[7]. These links, however, have limited capacity, and the information needs to be consequently quantized and sent over them. The limited-capacity fronthaul has been considered only for HD CF mMIMO systems in [8]–[10]. The distortion due to quantization is modeled in two different ways: i) as an additive noise term [9], [10]; and ii) as both attenuation and additive noise using the Bussgang decomposition for an optimal uniform quantizer [8]. Femenias *et al.* in [9] formulated a max-min uplink/downlink power allocation problem for HD CF mMIMO with limited-capacity fronthaul, while Masoumi *et al.* in [10] optimized the SE of a HD CF mMIMO uplink with limited-capacity fronthaul and hardware impairments. Bashar *et al.* in [8] derived the SE of HD CF mMIMO uplink with limited-capacity fronthaul. We consider the quantization-related limitations in the fronthaul of a FD CF mMIMO system to derive achievable SE expressions. To the best of our knowledge, ours is the first work to do so for a FD CF mMIMO system.

With tremendous increase in network traffic, the EE has become an important metric to design a modern wireless system. Global energy efficiency (GEE), defined as the ratio of the network SE and its total energy consumption, is being used to design CF mMIMO communication systems [11]–[14]. Ngo *et al.* in [11] optimized the GEE for the downlink of HD CF mMIMO system.

Bashar *et al.* in [12] optimized the uplink GEE of a HD CF mMIMO system with optimal uniform fronthaul quantization. Alonzo *et al.* in [13] optimized the GEE of CF and UE-centric HD mMIMO deployments in the mmWave regime. Nguyen *et al.* in [14] maximized a novel SE-GEE metric for the FD CF mMIMO system using the Dinkelbach-like algorithm.

A UE with limited energy availability will accord a much higher importance to its EE than an another UE with a sufficient energy supply. GEE is a network-centric metric and cannot accommodate such heterogeneous EE requirements of different UEs [15]. The weighted sum energy efficiency (WSEE) metric, defined as the weighted sum of individual EEs [15], can prioritize EEs of individual UEs, by allocating them a higher weight [16], [17]. Efrem *et al.* in [16] developed a systematic approach to maximize WSEE for a general wireless network. Sharma *et al.* in [17] maximized the WSEE of a two-way amplify-and-forward (AF) FD relay. The WSEE metric is yet to be investigated for CF mMIMO HD and FD systems.

Decentralized designs, which accomplish a complex task by coordination and cooperation of a set of computing units, are being used to design mMIMO systems [18], [19]. This interest is driven by high computational complexity and high interconnection data rate requirements between radio-frequency (RF) chains and baseband units (BBUs) in centralized mMIMO system designs [18]. Jeon *et al.* in [18] constructed decentralized equalizers by partitioning the BS antenna array. Reference [19] proposed a coordinate-descent-based decentralized algorithm for mMIMO uplink detection and downlink precoding. Reference [20] employed alternating direction method of multipliers (ADMM) to decentrally allocate edge-computing resource for vehicular networks. Reference [21] applied ADMM to decentrally maximize the WSEE for a two-way HD AF Relay. Such decentralized approaches have not yet been employed to optimize FD CF mMIMO systems. We next list our **main** contributions in this context:

- 1) We consider FD CF mMIMO communications with maximal ratio combining/maximal ratio transmission (MRC)/(MRT) processing and limited fronthaul with optimal uniform quantization. This is unlike the existing works on FD CF mMIMO [5]–[7], [14], which consider perfect high-capacity fronthaul links. We derive achievable SE expressions for both uplink and downlink UEs, which are valid for arbitrary number of antennas at each AP.

We use the derived SE expression to maximize the non-convex WSEE metric. While energy-efficient design of CF mMIMO systems have been studied in literature [11]–[14], most of them focus on the GEE metric, except reference [14]. The GEE, being a single ratio, can be

expressed as a pseudo-concave (PC) function and can thus be maximized using Dinkelbach's algorithm [15]. Reference [14] is the only work so far which optimized the EE of FD CF mMIMO. It considered a novel SE-GEE objective, which also reduces to a PC function and is maximized using a Dinkelbach-like algorithm. The WSEE, in contrast, is a sum of PC functions, and is not guaranteed to be a PC function [15]. This makes the WSEE an extremely non-trivial objective to maximize [15]. Further, the algorithm in [14] requires knowledge of instantaneous small-scale channel fading coefficients. The WSEE metric optimized here, in contrast, requires large-scale channel coefficients, which remains constant for multiple coherence intervals [2].

2) We decentrally maximize WSEE using a two-layered iterative approach combining successive convex approximation (SCA) and ADMM. The first layer first simplifies the non-convex WSEE maximization problem, by using epigraph transformation, slack variables and series approximations. It then locally approximates the problem as a generalized convex program (GCP) which is solved iteratively using the SCA approach. The second layer decentrally optimizes the GCP by using the consensus ADMM approach, which decomposes the centralized version into multiple sub-problems, each of which is solved independently. The local solutions are combined to obtain the global solution. We note that the GCP is not in the standard form which is required for applying ADMM, as it involves constraints that couple power control coefficients from different UEs. We therefore create global and local versions of the power control coefficients, which decouple the constraints, and iteratively update them till the algorithm converges.

3) We analytically and numerically prove the convergence of the proposed decentralized approach. We numerically demonstrate the tightness of our obtained achievable SE expressions and investigate its variation with various system model parameters. We numerically show that the proposed decentralized optimization i) achieves the same WSEE as the centralized approach; and ii) is responsive to changing weights which can be set to prioritize UEs' EE requirements. We numerically show that for high fronthaul capacity a higher number of fronthaul quantization bits is required to achieve high SE. This, however, reduces its WSEE. For low fronthaul capacity, a higher number of quantization bits achieves high SE and WSEE.

II. SYSTEM MODEL

We consider, as shown in Fig. 1, a FD CF mMIMO system where M FD APs serve K single-antenna HD UEs on the same spectral resource, comprising K_u UEs on the uplink and K_d UEs on the downlink, with $K = (K_u + K_d)$. Each AP has N_t transmit antennas and N_r

receive antennas, and is connected to the CPU using a limited-capacity fronthaul link which carries quantized uplink/downlink information to/from the CPU. From Fig. 1, due to FD model,

- uplink receive signal of each AP is interfered by its own downlink transmit signal (intra-AP) and that of other APs (inter-AP) (shown as purple (resp. brown) lines on (resp. between) APs).
- downlink UEs receive transmit signals from uplink UEs, causing uplink downlink interference (UDI) (shown as black dotted lines between uplink and downlink UEs). Additionally, the UEs experience multi-UE interference (MUI) as the APs serve them on the same spectral resource.

We next explain various channels, their estimation and data transmission. We assume a coherence interval of duration T_c (in s) with τ_c samples, which is divided into: a) channel estimation phase of τ_t samples, and b) downlink and uplink data transmission of $(\tau_c - \tau_t)$ samples.

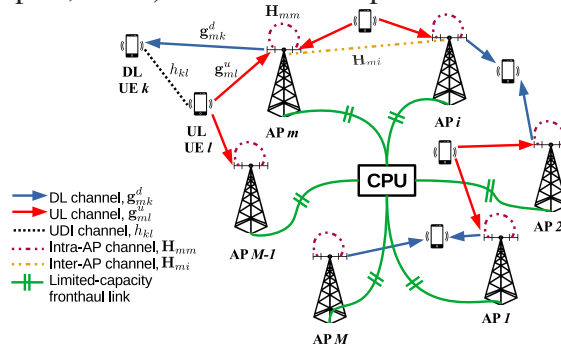


Fig. 1: System model for FD CF mMIMO communications

A. Channel description

The vector $\mathbf{g}_{mk}^d \in \mathbb{C}^{N_t \times 1}$ is the channel from the k th downlink UE to the transmit antennas of the m th AP, and $\mathbf{g}_{ml}^u \in \mathbb{C}^{N_r \times 1}$ is the channel from the l th uplink UE to the receive antennas of the m th AP¹. We model these channels as $\mathbf{g}_{mk}^d = (\beta_{mk}^d)^{1/2} \tilde{\mathbf{g}}_{mk}^d$ and $\mathbf{g}_{ml}^u = (\beta_{ml}^u)^{1/2} \tilde{\mathbf{g}}_{ml}^u$. Here β_{mk}^d and $\beta_{ml}^u \in \mathbb{R}$ are corresponding large scale fading coefficients, which are same for all antennas at the m th AP [2], [5]. The vectors $\tilde{\mathbf{g}}_{mk}^d$ and $\tilde{\mathbf{g}}_{ml}^u$ denote small scale fading with independent and identically distributed (i.i.d.) $\mathcal{CN}(0, 1)$ entries. The UDI channel between the k th downlink UE and l th uplink UE is modeled similar to [5], [6], as $h_{kl} = (\tilde{\beta}_{kl})^{1/2} \tilde{h}_{kl}$, where $\tilde{\beta}_{kl}$ is the large scale fading coefficient and $\tilde{h}_{kl} \sim \mathcal{CN}(0, 1)$ is the small scale fading. The inter- and intra-AP channels from the transmit antennas of the i th AP to the receive antennas of the m th AP are denoted as $\mathbf{H}_{mi} \in \mathbb{C}^{N_r \times N_t}$, $i = 1$ to M .

B. Uplink channel estimation

Pilot transmission: Recall that the channel estimation phase consists of τ_t samples. We divide them as $\tau_t = \tau_t^d + \tau_t^u$, where τ_t^d and τ_t^u are samples used as pilots for the downlink and uplink

¹We, henceforth, consider $k = 1$ to K_d , $l = 1$ to K_u and $m = 1$ to M , to avoid repetition, unless mentioned otherwise.

UEs, respectively. All the downlink (resp. uplink) UEs simultaneously transmit τ_t^d (resp. τ_t^u)-length uplink pilots to the APs, which they use to estimate the respective channels. In this phase, both transmit and receive antenna arrays of each AP, similar to [5], operate in receive mode. The k th downlink UE (resp. l th uplink UE) transmits pilot signals $\sqrt{\tau_t^d} \varphi_k^d \in \mathbb{C}^{\tau_t^d \times 1}$ (resp. $\sqrt{\tau_t^u} \varphi_l^u \in \mathbb{C}^{\tau_t^u \times 1}$). We assume, similar to [5], [11], that the pilots i) have unit norm i.e., $\|\varphi_l^u\| = \|\varphi_k^d\| = 1$; and ii) are intra-set orthonormal i.e. $(\varphi_l^u)^H \varphi_{l'}^u = 0 \forall l \neq l'$ and $(\varphi_k^d)^H \varphi_{k'}^d = 0 \forall k \neq k'$. Therefore, we need $\tau_t^d \geq K_d$ and $\tau_t^u \geq K_u$ [5], [11].

Pilot reception and channel estimation: The pilots received by the transmit and receive antennas of the m th AP are given respectively as

$$\mathbf{Y}_m^{tx} = \sqrt{\tau_t^d \rho_t} \sum_{k=1}^{K_d} \mathbf{g}_{mk}^d (\varphi_k^d)^H + \mathbf{W}_m^{tx}, \text{ and } \mathbf{Y}_m^{rx} = \sqrt{\tau_t^u \rho_t} \sum_{l=1}^{K_u} \mathbf{g}_{ml}^u (\varphi_l^u)^H + \mathbf{W}_m^{rx}.$$

Here ρ_t is the normalized pilot transmit signal-to-noise-ratio (SNR). The matrices $\mathbf{W}_m^{tx} \in \mathbb{C}^{N_t \times \tau_t^d}$ and $\mathbf{W}_m^{rx} \in \mathbb{C}^{N_r \times \tau_t^u}$ denote additive noise with $\mathcal{CN}(0, 1)$ entries. Each AP independently estimates its channels with the uplink and downlink UEs to avoid channel state information (CSI) exchange overhead [5], [14]. To estimate the channels \mathbf{g}_{mk}^d and \mathbf{g}_{ml}^u , the m th AP projects the received signal onto the pilot signals φ_k^d and φ_l^u respectively, as $\hat{\mathbf{g}}_{mk}^{tx} = \mathbf{Y}_m^{tx} \varphi_k^d = \sqrt{\tau_t^d \rho_t} \mathbf{g}_{mk}^d + \mathbf{W}_m^{tx} \varphi_k^d$ and $\hat{\mathbf{g}}_{ml}^{rx} = \mathbf{Y}_m^{rx} \varphi_l^u = \sqrt{\tau_t^u \rho_t} \mathbf{g}_{ml}^u + \mathbf{W}_m^{rx} \varphi_l^u$. These projections are used to compute the corresponding linear minimum-mean-squared-error (MMSE) channel estimates [5] as $\hat{\mathbf{g}}_{mk}^d = \mathbb{E}\{\mathbf{g}_{mk}^d (\hat{\mathbf{g}}_{mk}^{tx})^H\} (\mathbb{E}\{\hat{\mathbf{g}}_{mk}^{tx} (\hat{\mathbf{g}}_{mk}^{tx})^H\})^{-1} \hat{\mathbf{g}}_{mk}^{tx}$, $\hat{\mathbf{g}}_{ml}^u = \mathbb{E}\{\mathbf{g}_{ml}^u (\hat{\mathbf{g}}_{ml}^{rx})^H\} (\mathbb{E}\{\hat{\mathbf{g}}_{ml}^{rx} (\hat{\mathbf{g}}_{ml}^{rx})^H\})^{-1} \hat{\mathbf{g}}_{ml}^{rx} = c_{ml}^u \hat{\mathbf{g}}_{ml}^{rx}$, where $c_{mk}^d = \frac{\sqrt{\tau_t^d \rho_t} \beta_{mk}^d}{\tau_t^d \rho_t \beta_{mk}^d + 1}$ and $c_{ml}^u = \frac{\sqrt{\tau_t^u \rho_t} \beta_{ml}^u}{\tau_t^u \rho_t \beta_{ml}^u + 1}$. The estimation error vectors are defined as $\mathbf{e}_{ml}^u \triangleq \mathbf{g}_{ml}^u - \hat{\mathbf{g}}_{ml}^u$ and $\mathbf{e}_{mk}^d \triangleq \mathbf{g}_{mk}^d - \hat{\mathbf{g}}_{mk}^d$. With MMSE channel estimation, $\hat{\mathbf{g}}_{mk}^d$, \mathbf{e}_{mk}^d and $\hat{\mathbf{g}}_{ml}^u$, \mathbf{e}_{ml}^u are mutually independent and their individual terms are i.i.d. with pdf $\mathcal{CN}(0, \gamma_{mk}^d)$, $\mathcal{CN}(0, \beta_{mk}^d - \gamma_{mk}^d)$, $\mathcal{CN}(0, \gamma_{ml}^u)$, $\mathcal{CN}(0, \beta_{ml}^u - \gamma_{ml}^u)$ respectively, with $\gamma_{mk}^d = \frac{\tau_t^d \rho_t (\beta_{mk}^d)^2}{\tau_t^d \rho_t \beta_{mk}^d + 1}$ and $\gamma_{ml}^u = \frac{\tau_t^u \rho_t (\beta_{ml}^u)^2}{\tau_t^u \rho_t \beta_{ml}^u + 1}$ [5], [11]. After channel estimation, data transmission starts simultaneously on downlink and uplink.

C. Transmission model

An objective of this work is to derive a SE lower bound for FD CF mMIMO systems, where the M APs serve K_u uplink UEs and K_d downlink UEs simultaneously on the same spectral resource. We note that for the FD CF mMIMO systems, unlike the HD CF mMIMO systems [2], [8], [9], uplink and downlink transmissions interfere to cause UDI and inter-/intra-AP interferences. Further, unlike existing FD CF mMIMO literature [5], [6], [14], we consider a limited-capacity fronthaul. It is critical to model and analyze the UDI and inter-/intra-AP interferences and limited-capacity impairments while deriving the lower bound.

1) *Downlink data transmission:* The CPU chooses a message symbol s_k^d for the k th downlink UE, which is distributed as $\mathcal{CN}(0, 1)$. It intends to send this symbol to the m th AP via the limited-capacity fronthaul link. Before doing that, it multiplies s_k^d with a power-control coefficient η_{mk} , and then quantizes the resulting signal. The m th AP, due to its limited fronthaul capacity, is allowed to serve only a subset $\kappa_{dm} \subset \{1, \dots, K_d\}$ of downlink users, an aspect which is discussed later in Section II-D. The CPU consequently sends downlink symbols for UEs in the set κ_{dm} to the m th AP, which uses MMSE channel estimates to perform MRT precoding. The transmit signal of m th AP is therefore given as follows

$$\mathbf{x}_m^d = \sqrt{\rho_d} \sum_{k \in \kappa_{dm}} (\hat{\mathbf{g}}_{mk}^d)^* \mathcal{Q}(\sqrt{\eta_{mk}} s_k^d) = \sqrt{\rho_d} \sum_{k \in \kappa_{dm}} (\hat{\mathbf{g}}_{mk}^d)^* (\tilde{a} \sqrt{\eta_{mk}} s_k^d + \varsigma_{mk}^d). \quad (1)$$

Here ρ_d is the normalized maximum transmit SNR at each AP. The function $\mathcal{Q}(\cdot)$ denotes the quantization operation, which is modeled as a multiplicative attenuation, \tilde{a} , and an additive distortion, ς_{mk}^d , for the k th downlink UE in the fronthaul link between the CPU and the m th AP [8], [12]. We have, from Appendix A, $\mathbb{E}\{(\varsigma_{mk}^d)^2\} = (\tilde{b} - \tilde{a}^2) \mathbb{E}\{|\sqrt{\eta_{mk}} s_k^d|^2\} = (\tilde{b} - \tilde{a}^2) \eta_{mk}$. As explained in Appendix A, \tilde{a} and \tilde{b} depend on the number of fronthaul quantization bits. The m th AP satisfies the average transmit SNR constraint, $\mathbb{E}\{\|\mathbf{x}_m^d\|^2\} \leq \rho_d$, as follows

$$\rho_d \tilde{b} \sum_{k \in \kappa_{dm}} \eta_{mk} \mathbb{E}\{\|\hat{\mathbf{g}}_{mk}^d\|^2\} \leq \rho_d \Rightarrow \tilde{b} \sum_{k \in \kappa_{dm}} \eta_{mk} \leq \frac{1}{N_t}. \quad (2)$$

The k th downlink UE receives its desired message signal from a subset of all APs, denoted as $\mathcal{M}_k^d \subset \{1, \dots, M\}$, along with various interference and distortion components, as follows

$$\begin{aligned} r_k^d &= \sum_{m=1}^M (\mathbf{g}_{mk}^d)^T \mathbf{x}_m^d + \sum_{l=1}^{K_u} h_{kl} x_l^u + w_k^d \\ &= \underbrace{\tilde{a} \sqrt{\rho_d} \sum_{m \in \mathcal{M}_k^d} \sqrt{\eta_{mk}} (\mathbf{g}_{mk}^d)^T (\hat{\mathbf{g}}_{mk}^d)^* s_k^d}_{\text{message signal}} + \underbrace{\tilde{a} \sqrt{\rho_d} \sum_{m=1}^M \sum_{q \in \kappa_{dm} \setminus k} \sqrt{\eta_{mq}} (\mathbf{g}_{mk}^d)^T (\hat{\mathbf{g}}_{mq}^d)^* s_q^d}_{\text{multi-UE interference, MUI}_k^d} \\ &\quad + \underbrace{\sum_{l=1}^{K_u} h_{kl} x_l^u}_{\text{uplink downlink interference, UDI}_k^d} + \underbrace{\sqrt{\rho_d} \sum_{m=1}^M \sum_{q \in \kappa_{dm}} (\mathbf{g}_{mk}^d)^T (\hat{\mathbf{g}}_{mq}^d)^* \varsigma_{mq}^d}_{\text{total quantization distortion, TQD}_k^d} + \underbrace{w_k^d}_{\text{AWGN at receiver}}. \quad (3) \end{aligned}$$

The m th AP serves the k th downlink UE iff $k \in \kappa_{dm} \Leftrightarrow m \in \mathcal{M}_k^d$. Here x_l^u is the transmit signal of the l th uplink UE, which is discussed and modelled below.

2) *Uplink data transmission:* The K_u uplink UEs also simultaneously transmit to all M APs on the same spectral resource as that of the K_d downlink UEs. The l th uplink UE transmits

its signal $x_l^u = \sqrt{\rho_u \theta_l} s_l^u$ with s_l^u being its message symbol with pdf $\mathcal{CN}(0, 1)$, ρ_u being the maximum uplink transmit SNR and θ_l being the power control coefficient. To satisfy the average SNR constraint, $\mathbb{E}\{|x_l^u|^2\} \leq \rho_u$, the l th uplink UE satisfies the following constraint

$$0 \leq \theta_l \leq 1. \quad (4)$$

The FD APs not only receive uplink UE signals but also their own downlink transmit signals and that of the other APs, referred to as intra-AP and inter-AP interference, respectively. Using (1), the received uplink signal at the m th AP is expressed as

$$\mathbf{y}_m^u = \sum_{l=1}^{K_u} \mathbf{g}_{ml}^u x_l^u + \sum_{i=1}^M \mathbf{H}_{mi} \mathbf{x}_i^d + \mathbf{w}_m^u = \sqrt{\rho_u} \sum_{l=1}^{K_u} \mathbf{g}_{ml}^u \sqrt{\theta_l} s_l^u + \sqrt{\rho_d} \sum_{i=1}^M \sum_{k \in \kappa_{di}} \mathbf{H}_{mi} (\hat{\mathbf{g}}_{ik}^d)^* (\tilde{a} \sqrt{\eta_{ik}} s_k^d + \varsigma_{ik}^d) + \mathbf{w}_m^u. \quad (5)$$

Here $\mathbf{w}_m^u \in \mathbb{C}^{N_r \times 1}$ is the additive receiver noise at the m th AP with i.i.d. entries $\sim \mathcal{CN}(0, 1)$.

The intra and inter-AP interference channels vary extremely slowly and the FD APs can thus estimate them with very low pilot overhead [6]. We assume that these channel estimates are imperfect. The receive antenna array of each AP, similar to [5], [6], can therefore only partially mitigate the intra- and inter-AP interference. The residual intra-/inter-AP interference (RI) channel $\mathbf{H}_{mi} \in \mathbb{C}^{N_r \times N_t}$, $i = 1$ to M after suppression, similar to [4]–[6], [17], is modeled as Rayleigh faded with entries i.i.d. $\sim \mathcal{CN}(0, \gamma_{\text{RI}, mi})$. Here $\gamma_{\text{RI}, mi} \triangleq \beta_{\text{RI}, mi} \gamma_{\text{RI}}$, with $\beta_{\text{RI}, mi}$ being the large scale fading coefficient from the i th AP to the m th AP, and γ_{RI} being the RI power after interference cancellation.

The m th AP receives the signals from all the uplink UEs, and performs MRC for the l th uplink UE with $(\hat{\mathbf{g}}_{ml}^u)^H$. Due to the limited fronthaul capacity: i) AP quantizes the combined signal before sending it to CPU; ii) as discussed in detail later in Section II-D, the CPU receives contributions for the l th uplink UE only from the subset of APs serving it, denoted as $\mathcal{M}_l^u \subset \{1, \dots, M\}$. Using (5), the signal received by the CPU for the l th uplink UE is expressed as

$$\begin{aligned} r_l^u = & \sum_{m \in \mathcal{M}_l^u} \mathcal{Q}((\hat{\mathbf{g}}_{ml}^u)^H \mathbf{y}_m^u) = \underbrace{\tilde{a} \sum_{m \in \mathcal{M}_l^u} \sqrt{\rho_u} \sqrt{\theta_l} (\hat{\mathbf{g}}_{ml}^u)^H \mathbf{g}_{ml}^u s_l^u}_{\text{message signal}} + \underbrace{\tilde{a} \sum_{m \in \mathcal{M}_l^u} \sum_{\substack{q=1 \\ q \neq l}}^{K_u} \sqrt{\rho_u} \sqrt{\theta_q} (\hat{\mathbf{g}}_{ml}^u)^H \mathbf{g}_{mq}^u s_q^u}_{\text{multi-UE interference, MUI}_l^u} \\ & + \underbrace{\tilde{a} \sum_{m \in \mathcal{M}_l^u} \sum_{i=1}^M \sqrt{\rho_d} \sum_{k \in \kappa_{di}} (\hat{\mathbf{g}}_{ml}^u)^H \mathbf{H}_{mi} (\hat{\mathbf{g}}_{ik}^d)^* (\tilde{a} \sqrt{\eta_{ik}} s_k^d + \varsigma_{ik}^d)}_{\text{residual interference (intra-AP and inter-AP), RI}_l^u} + \underbrace{\tilde{a} \sum_{m \in \mathcal{M}_l^u} (\hat{\mathbf{g}}_{ml}^u)^H \mathbf{w}_m^u}_{\text{AWGN at APs, N}_l^u} + \underbrace{\sum_{m \in \mathcal{M}_l^u} \varsigma_{ml}^u}_{\text{total quantization distortion, TQD}_l^u}. \quad (6) \end{aligned}$$

We denote the subset of uplink UEs served by the m th AP as $\kappa_{um} \subset \{1, \dots, K_u\}$. The m th AP serves the l th uplink UE iff $l \in \kappa_{um} \Leftrightarrow m \in \mathcal{M}_l^u$. The quantization operation $\mathcal{Q}(\cdot)$ is mathematically modeled using constant attenuation \tilde{a} , and additive distortion ς_{ml}^u which, as shown in Appendix A, has power $\mathbb{E}\{(\varsigma_{ml}^u)^2\} = (\tilde{b} - \tilde{a}^2)\mathbb{E}\left\{|(\mathbf{g}_{ml}^u)^H \mathbf{y}_m|^2\right\}$.

D. Quantization, limited fronthaul and AP selection

The fronthaul between the m th AP and the CPU uses ν_m bits to quantize the real and imaginary parts of transmit signal of the m th downlink UE and the uplink receive signal after MRC i.e., $\sqrt{\eta_{mk}}s_k^d$, and $(\hat{\mathbf{g}}_{ml}^u)^H \mathbf{y}_m^u$, respectively. Due to the limited-capacity fronthaul, the m th AP serves only $K_{um} (\triangleq |\kappa_{um}|)$ and $K_{dm} (\triangleq |\kappa_{dm}|)$ UEs on the uplink and downlink, respectively [8], [12]. For each UE, we recall that there are $(\tau_c - \tau_t)$ data samples in each coherence interval of duration T_c . The fronthaul data rate between the m th AP and the CPU, in bps (bits per second), is

$$R_{\text{fh},m} = \frac{2\nu_m(K_{dm} + K_{um})(\tau_c - \tau_t)}{T_c}. \quad (7)$$

The fronthaul link between the m th AP and the CPU has capacity $C_{\text{fh},m}$ which implies that

$$R_{\text{fh},m} \leq C_{\text{fh},m} \Rightarrow \nu_m \cdot (K_{um} + K_{dm}) \leq \frac{C_{\text{fh},m}T_c}{2(\tau_c - \tau_t)}. \quad (8)$$

To maximize K_{um} , it is possible to set $K_{dm} = 0$, and vice-versa. However, to ensure uplink and downlink fairness for the FD system, we set the same maximum limit to the number of uplink as well as downlink UEs an AP can serve, which satisfies (8). We arrive at the following lemma.

Lemma 1. The maximum number of uplink and downlink UEs served by the m th AP when connected via a limited optical fronthaul to the CPU with capacity $C_{\text{fh},m}$ is given as

$$\bar{K}_{um} = \bar{K}_{dm} = \left\lfloor \frac{C_{\text{fh},m}T_c}{4(\tau_c - \tau_t)\nu_m} \right\rfloor. \quad (9)$$

Proof: Let \bar{K}_{um} and \bar{K}_{dm} denote the maximum number of uplink and downlink UEs served by the m th AP. We consider $\bar{K}_{um} = \bar{K}_{dm}$ for uplink and downlink fairness. Using (8), we get,

$$\bar{K}_{um} = \bar{K}_{dm} \leq \frac{C_{\text{fh},m}T_c}{4(\tau_c - \tau_t)\nu_m}.$$

The lemma follows directly from the definition of floor function $\lfloor \cdot \rfloor$. ■

Using the maximum limits obtained in (9), we assign $K_{um} = \min\{K_u, \bar{K}_{um}\}$ and $K_{dm} = \min\{K_d, \bar{K}_{dm}\}$. We see that the constraint imposed in (8) is similar to a UE-centric (UC) CF mMIMO system, wherein each UE is served by a subset of the APs [3]. We now define the procedure for AP selection to obtain the best subset of APs to serve each uplink and downlink UE, while satisfying (8). For this, we extend the procedure in [8] for a FD system as follows:

- The m th AP sorts the uplink and downlink UEs connected to it in descending order based on

their channel gains (β_{ml}^u and β_{mk}^d , respectively) and chooses K_{um} uplink UEs and K_{dm} downlink UEs, with the largest channel gains, to populate the sets κ_{um} and κ_{dm} , respectively.

- For the l th uplink UE and the k th downlink UE, we populate the sets \mathcal{M}_l^u and \mathcal{M}_k^d , respectively, using the axioms $l \in \kappa_{um} \Leftrightarrow m \in \mathcal{M}_l^u$ and $k \in \kappa_{dm} \Leftrightarrow m \in \mathcal{M}_k^d$.
- If an uplink or downlink UE is found with no serving AP, we the procedure in Algorithm 1 to assign it the AP with the best channel conditions, while satisfying (8).

Algorithm 1: Fair AP selection for disconnected uplink and downlink UEs

```

1 for  $k \leftarrow 1$  to  $K_d$  do
2   if  $\mathcal{M}_k^d = \phi$  then
     Sort the APs in descending order of channel gains,  $\beta_{mk}^d$ , and find the AP  $n$  with the largest channel gain.
     For this  $n$ th AP, sort downlink UEs in  $\kappa_{dn}$  in descending order of channel gains and find the  $q$ th downlink UE
     with minimum channel gain and at least one more connected AP.
     Remove the  $q$ th downlink UE from the set  $\kappa_{dn}$  and add the  $k$ th downlink UE to it.
3 Repeat the same procedure for all the uplink UEs  $l = 1$  to  $K_u$ .
```

III. ACHIEVABLE SPECTRAL EFFICIENCY

We now derive the ergodic SE for the k th downlink UE and the l th uplink UE, denoted respectively as \bar{S}_k^d and \bar{S}_l^u . The AP employs MRC in the uplink, and MRT in the downlink, and optimal uniform quantization in the fronthaul. The ergodic SE expressions are calculated using (3) and (6), as follows

$$\bar{S}_\phi^\varepsilon = \left(\frac{\tau_c - \tau_t}{\tau_c} \right) \mathbb{E} \left\{ \log_2 \left(1 + \frac{P_\phi^\varepsilon}{I_\phi^\varepsilon + (\sigma_{\phi,0}^\varepsilon)^2} \right) \right\}, \text{ where} \quad (10)$$

$$P_\phi^\varepsilon = \left| \tilde{a} \sum_{m \in \mathcal{M}_\phi^\varepsilon} \sqrt{\rho_\varepsilon} \sqrt{v_{m\phi}^\varepsilon} (\hat{\mathbf{g}}_{m\phi}^\varepsilon)^H \mathbf{g}_{m\phi}^\varepsilon s_\phi^\varepsilon \right|^2, (\sigma_{l,0}^u)^2 = \left| \tilde{a} \sum_{m \in \mathcal{M}_l^u} (\hat{\mathbf{g}}_{ml}^u)^H \mathbf{w}_m^u \right|^2, (\sigma_{k,0}^d)^2 = |w_k^d|^2,$$

$$\begin{aligned}
I_l^u &= \left| \tilde{a} \sum_{m \in \mathcal{M}_l^u} \sum_{\substack{q=1 \\ q \neq l}}^{K_u} \sqrt{\rho_u} \sqrt{\theta_q} (\hat{\mathbf{g}}_{ml}^u)^H \mathbf{g}_{mq}^u s_q^u \right|^2 \\
&+ \left| \tilde{a} \sum_{m \in \mathcal{M}_l^u} \sum_{i=1}^M \sqrt{\rho_d} \sum_{k \in \kappa_{di}} (\hat{\mathbf{g}}_{ml}^u)^H \mathbf{H}_{mi} (\hat{\mathbf{g}}_{ik}^d)^* (\tilde{a} \sqrt{\eta_{ik}} s_k^d + \varsigma_{ik}^d) \right|^2 + \left| \sum_{m \in \mathcal{M}_l^u} \varsigma_{ml}^u \right|^2, \\
I_k^d &= \left| \sum_{l=1}^{K_u} h_{kl} \sqrt{\rho_u} \theta_l s_l^u \right|^2 + \left| \tilde{a} \sqrt{\rho_d} \sum_{m=1}^M \sum_{q \in \kappa_{dm} \setminus k} \sqrt{\eta_{mq}} (\mathbf{g}_{mk}^d)^T (\hat{\mathbf{g}}_{mq}^d)^* s_q^d \right|^2 \\
&+ \left| \sqrt{\rho_d} \sum_{m=1}^M \sum_{q \in \kappa_{dm}} (\mathbf{g}_{mk}^d)^T (\hat{\mathbf{g}}_{mq}^d)^* \varsigma_{mq}^d \right|^2,
\end{aligned}$$

are signal, noise and interference powers, respectively, for the l th uplink and k th downlink UEs. We use $\varepsilon \triangleq \{d, u\}$ to denote downlink and uplink, respectively; $\phi \triangleq \{k, l\}$ to denote k th downlink UE and l th uplink UE, respectively; and $v_{m\phi}^\varepsilon \triangleq \{\eta_{mk}$ for $\phi = k, \theta_l$ for $\phi = l\}$. The expectation outside logarithm in the SE expressions in (10) is mathematically intractable, and it is difficult to simplify them further [2], [5], [8]. We, similar to [2], employ use-and-then-forget (UatF) technique to derive SE lower bounds. To use UatF, we rewrite the received signal at the CPU for the l th uplink UE in (6), and at the k th downlink UE in (3), as

$$r_\phi^\varepsilon = \underbrace{\tilde{a} \sum_{m \in \mathcal{M}_\phi^\varepsilon} \sqrt{\rho_\varepsilon} \sqrt{v_{m\phi}^\varepsilon} \mathbb{E}\{(\hat{\mathbf{g}}_{m\phi}^\varepsilon)^H \mathbf{g}_{m\phi}^\varepsilon\}}_{\text{desired signal, DS}_\phi^\varepsilon} s_\phi^\varepsilon + n_\phi^\varepsilon, \quad (11)$$

where the effective additive noise terms n_ϕ^ε are expressed as follows:

$$\begin{aligned} n_l^u &= \underbrace{\tilde{a} \sqrt{\rho_u} \sqrt{\theta_l} \sum_{m \in \mathcal{M}_l^u} ((\hat{\mathbf{g}}_{ml}^u)^H \mathbf{g}_{ml}^u - \mathbb{E}\{(\hat{\mathbf{g}}_{ml}^u)^H \mathbf{g}_{ml}^u\}) s_l^u}_{\text{beamforming uncertainty, BU}_l^u} + \underbrace{\tilde{a} \sum_{m \in \mathcal{M}_l^u} \sum_{\substack{q=1 \\ q \neq l}}^{K_u} \sqrt{\rho_u} \sqrt{\theta_q} (\hat{\mathbf{g}}_{ml}^u)^H \mathbf{g}_{mq}^u s_q^u}_{\text{MUI}_l^u} \\ &+ \underbrace{\tilde{a} \sum_{m \in \mathcal{M}_l^u} \sum_{i=1}^M \sqrt{\rho_d} \sum_{k \in \kappa_{di}} (\hat{\mathbf{g}}_{ml}^u)^H \mathbf{H}_{mi} (\hat{\mathbf{g}}_{ik}^d)^* (\tilde{a} \sqrt{\eta_{ik}} s_k^d + \varsigma_{ik}^d)}_{\text{RI}_l^u} + \underbrace{\tilde{a} \sum_{m \in \mathcal{M}_l^u} (\hat{\mathbf{g}}_{ml}^u)^H \mathbf{w}_m}_{N_l^u} + \underbrace{\sum_{m \in \mathcal{M}_l^u} \varsigma_{ml}^u}_{\text{TQD}_l^u}, \quad (12) \\ n_k^d &= \underbrace{\tilde{a} \sqrt{\rho_d} \sum_{m \in \mathcal{M}_k^d} \sqrt{\eta_{mk}} ((\mathbf{g}_{mk}^d)^T (\hat{\mathbf{g}}_{mk}^d)^* - \mathbb{E}\{(\mathbf{g}_{mk}^d)^T (\hat{\mathbf{g}}_{mk}^d)^*\}) s_k^d}_{\text{beamforming uncertainty, BU}_k^d} + \underbrace{\sqrt{\rho_u} \sum_{l=1}^{K_u} h_{kl} \sqrt{\theta_l} s_l^u}_{\text{UDI}_k^d} \\ &+ \underbrace{\tilde{a} \sqrt{\rho_d} \sum_{m=1}^M \sum_{q \in \kappa_{dm} \setminus k} \sqrt{\eta_{mq}} (\mathbf{g}_{mk}^d)^T (\hat{\mathbf{g}}_{mq}^d)^* s_q^d}_{\text{MUI}_k^d} + \underbrace{\sqrt{\rho_d} \sum_{m=1}^M \sum_{q \in \kappa_{dm}} (\mathbf{g}_{mk}^d)^T (\hat{\mathbf{g}}_{mq}^d)^* \varsigma_{mq}^d + w_k^d}_{\text{TQD}_k^d}. \quad (13) \end{aligned}$$

The term $\text{DS}_\phi^\varepsilon$ in (11) denotes the “true” desired signal received over the channel mean, and the term $\text{BU}_\phi^\varepsilon$ in (12)-(13) denotes beamforming uncertainty, a “signal leakage” term received over deviation of channel from mean. It is easy to see that n_ϕ^ε are uncorrelated with their respective $\text{DS}_\phi^\varepsilon$ terms. We, similar to [5], treat them as worst-case additive Gaussian noise. The central limit theorem guarantees that this approximation is tight for massive MIMO systems [5]. Using (11)-(13), we derive an achievable SE lower bound for each UE and state the following theorem.

Theorem 1. An achievable lower bound to the SE for the k th downlink UE with MRT and the

l th uplink UE with MRC can be expressed respectively as

$$S_k^d(\boldsymbol{\eta}, \boldsymbol{\Theta}, \boldsymbol{\nu}) = \tau_f \log_2 \left(1 + \frac{(\sum_{m \in \mathcal{M}_k^d} A_{mk}^d \sqrt{\eta_{mk}})^2}{\sum_{m=1}^M \sum_{q \in \kappa_{dm}} B_{kmq}^d \eta_{mq} + \sum_{l=1}^{K_u} D_{kl}^d \theta_l + 1} \right), \quad (14)$$

$$S_l^u(\boldsymbol{\eta}, \boldsymbol{\Theta}, \boldsymbol{\nu}) = \tau_f \log_2 \left(1 + \frac{A_l^u \theta_l}{\sum_{q=1}^{K_u} B_{lq}^u \theta_q + \sum_{i=1}^M \sum_{k \in \kappa_{di}} D_{lik}^u \eta_{ik} + E_l^u \theta_l + F_l^u} \right), \quad (15)$$

where $\tau_f = \left(\frac{\tau_c - \tau_t}{\tau_c} \right)$, $A_l^u = \tilde{a}^2 N_r^2 \rho_u \left(\sum_{m \in \mathcal{M}_l^u} \gamma_{ml}^u \right)^2$, $B_{lq}^u = \tilde{b} N_r \rho_u \sum_{m \in \mathcal{M}_l^u} \gamma_{ml}^u \beta_{mq}^u$, $D_{lik}^u = \tilde{b}^2 N_r N_t \rho_d \gamma_{ik}^d \sum_{m \in \mathcal{M}_l^u} \gamma_{ml}^u \beta_{li,mi} \gamma_{li}$, $E_l^u = (\tilde{b} - \tilde{a}^2) N_r^2 \rho_u \sum_{m \in \mathcal{M}_l^u} (\gamma_{ml}^u)^2$, $F_l^u = \tilde{b} N_r \sum_{m \in \mathcal{M}_l^u} \gamma_{ml}^u$, $A_{mk}^d = \tilde{a} N_t \sqrt{\rho_d} \gamma_{mk}^d$, $B_{kmq}^d = \tilde{b} N_t \rho_d \beta_{mk}^d \gamma_{mq}^d$ and $D_{kl}^d = \rho_u \tilde{\beta}_{kl}$. Here $\boldsymbol{\eta} \triangleq \{\eta_{mk}\} \in \mathbb{C}^{M \times K_d}$, $\boldsymbol{\Theta} \triangleq \{\theta_l\} \in \mathbb{C}^{K_u \times 1}$ and $\boldsymbol{\nu} \triangleq \{\nu_m\} \in \mathbb{C}^{M \times 1}$ are the variables on which the SE is dependent. We recall from Section II that \tilde{a} and \tilde{b} in (14)-(15) depend on the number of quantization bits, $\boldsymbol{\nu}$.

Proof: Refer to Appendix B. This proof simplifies the uplink downlink interference, UDI_k^d , and the residual intra- and inter-AP interference, RI_l^u , terms. We see that the SE expressions are functions of large scale fading coefficients, γ_{mk}^d and γ_{ml}^u . We will use them to optimize WSEE. *This is unlike [14] which requires instantaneous channel while optimizing SE-GEE metric.* ■

IV. TWO-LAYER DECENTRALIZED WSEE OPTIMIZATION FOR FD CF MMIMO

We now devise a decentralized algorithm which maximizes WSEE by calculating the optimal downlink and uplink power control coefficients $\boldsymbol{\eta}^*$ and $\boldsymbol{\Theta}^*$, respectively. We denote $\varepsilon \triangleq \{d, u\}$ for the downlink and uplink, respectively; $\phi \triangleq \{k, l\}$ for the k th downlink UE and l th uplink UE, respectively; and first define the individual EE for each UE as $\text{EE}_\phi^\varepsilon = \frac{B \cdot S_\phi^\varepsilon}{p_\phi^\varepsilon}$ [16], where B is the system bandwidth, and p_ϕ^ε denotes the power consumed by each UE. The power consumed by the k th downlink UE and the l th uplink UE are given as, respectively [12], [14]

$$p_k^d = P_{\text{fix}} + N_t \rho_d N_0 \sum_{m \in \mathcal{M}_k^d} \frac{1}{\alpha_m} \gamma_{mk}^d \eta_{mk} + P_{\text{tc},k}^d, \text{ and } p_l^u = P_{\text{fix}} + \rho_u N_0 \frac{1}{\alpha_l'} \theta_l + P_{\text{tc},l}^u. \quad (16)$$

Here α_m and α_l' are power amplifier efficiencies at the m th AP and the l th uplink UE respectively [5], N_0 is the noise power and $P_{\text{tc},k}^d$ and $P_{\text{tc},l}^u$ are the powers required to run the transceiver chains at each antenna of the k th downlink UE and the l th uplink UE, respectively. P_{fix} is the power consumed by the AP transceiver chains and the fronthaul between the APs and the CPU:

$$P_{\text{fix}} = \frac{1}{(K_u + K_d)} \sum_{m=1}^M \left(P_{0,m} + (N_t + N_r) P_{\text{tc},m} + P_{\text{ft}} \frac{R_{\text{fh},m}}{C_{\text{fh},m}} \right). \quad (17)$$

Here $P_{\text{tc},m}$ is the power required to run the transceiver chains at each antenna of the m th AP. The fronthaul power consumption for the m th AP has a fixed component, $P_{0,m}$, and a traffic-dependent component, which attains a maximum value of P_{ft} at full capacity $C_{\text{fh},m}$. The term

$R_{\text{fh},m}$, given in (7), is the fronthaul data rate of the m th AP.

The WSEE is now defined as the weighted sum of individual EEs of different users [15], as

$$\text{WSEE} = \sum_{k=1}^{K_d} w_k^d \text{EE}_k^d + \sum_{l=1}^{K_u} w_l^u \text{EE}_l^u \triangleq B \left(\sum_{k=1}^{K_d} w_k^d \frac{S_k^d(\boldsymbol{\eta}, \boldsymbol{\Theta}, \boldsymbol{\nu})}{p_k^d(\boldsymbol{\eta}, \boldsymbol{\nu})} + \sum_{l=1}^{K_u} w_l^u \frac{S_l^u(\boldsymbol{\eta}, \boldsymbol{\Theta}, \boldsymbol{\nu})}{p_l^u(\boldsymbol{\Theta}, \boldsymbol{\nu})} \right), \quad (18)$$

where w_ϕ^ε are weights assigned to the UEs to account for their heterogeneous EE requirements.

The WSEE metric can prioritize the EE requirements of individual UEs by assigning them different weights [16], [17]. For example, it could assign a higher weight to a UE that is more energy-scarce. The WSEE maximization problem can now be formulated as follows

$$\begin{aligned} \mathbf{P1} : \max_{\boldsymbol{\eta}, \boldsymbol{\Theta}, \boldsymbol{\nu}} \quad & B \left(\sum_{k=1}^{K_d} w_k^d \frac{S_k^d(\boldsymbol{\eta}, \boldsymbol{\Theta}, \boldsymbol{\nu})}{p_k^d(\boldsymbol{\eta}, \boldsymbol{\nu})} + \sum_{l=1}^{K_u} w_l^u \frac{S_l^u(\boldsymbol{\eta}, \boldsymbol{\Theta}, \boldsymbol{\nu})}{p_l^u(\boldsymbol{\Theta}, \boldsymbol{\nu})} \right) \\ \text{s.t.} \quad & S_k^d(\boldsymbol{\eta}, \boldsymbol{\Theta}, \boldsymbol{\nu}) \geq S_{ok}^d, S_l^u(\boldsymbol{\eta}, \boldsymbol{\Theta}, \boldsymbol{\nu}) \geq S_{ol}^u, \end{aligned} \quad (19a)$$

$$R_{\text{fh},m} \leq C_{\text{fh},m}, (2), (4). \quad (19b)$$

The quality-of-service (QoS) constraints in (19a) guarantee a minimum SE, denoted by the constants S_{ok}^d and S_{ol}^u , for each downlink and uplink UE respectively. The first constraint in (19b) ensures that the fronthaul transmission rate for all APs is within the capacity limit. We observe that the number of quantization bits $\boldsymbol{\nu}$, if included in problem **P1**, will make it a difficult-to-solve integer optimization problem [8], [12], [22]. We therefore solve it to optimize the power control coefficients $\{\boldsymbol{\eta}, \boldsymbol{\Theta}\}$, by fixing $\boldsymbol{\nu}$ such that it satisfies the first constraint in (19b) [8], [12], and numerically investigate $\boldsymbol{\nu}$ in Section V. We omit the constant B and reformulate **P1** as follows

$$\begin{aligned} \mathbf{P2} : \max_{\boldsymbol{\eta}, \boldsymbol{\Theta}} \quad & \sum_{k=1}^{K_d} w_k^d \frac{S_k^d(\boldsymbol{\eta}, \boldsymbol{\Theta})}{p_k^d(\boldsymbol{\eta})} + \sum_{l=1}^{K_u} w_l^u \frac{S_l^u(\boldsymbol{\eta}, \boldsymbol{\Theta})}{p_l^u(\boldsymbol{\Theta})} \\ \text{s.t.} \quad & S_k^d(\boldsymbol{\eta}, \boldsymbol{\Theta}) \geq S_{ok}^d, S_l^u(\boldsymbol{\eta}, \boldsymbol{\Theta}) \geq S_{ol}^u, \\ & (2), (4). \end{aligned} \quad (20)$$

The objective in **P2** is a sum of ratios, each of which is a PC function (concave-over-linear) of power control coefficients $\{\boldsymbol{\eta}, \boldsymbol{\Theta}\}$. It is, therefore, not guaranteed to be a PC function and Dinkelbach's algorithm, cannot be applied to maximize it [15]. This makes it a much harder objective to optimize as opposed to the more commonly studied GEE metric, which is a PC function [15] and has been investigated for CF mMIMO systems [11]–[14].

We now maximize WSEE centrally and decentrally using a two-layered approach. The first layer comprises an SCA framework, which formulates a GCP by approximating the non-convex

objective and constraints in **P2** as convex. In the second layer, the approximate GCP formed in the n th SCA iteration is either solved centrally or decentrally using ADMM. Since the approximate GCP obtained in the first layer, due to coupled optimization variables, is not in the standard ADMM form, we introduce their local and global versions. The sub-problems to update local variables are solved independently, and the local variables are coordinated to calculate the global solution [20], [21], [23]. The updation of variables and coordination continues till ADMM converges. The obtained solution is then used to formulate GCP for $(n + 1)$ th SCA iteration.

A. SCA Framework

We now first linearize the non-convex objective in **P2** using epigraph transformation as [22]

$$\begin{aligned} \mathbf{P3} : \quad & \max_{\boldsymbol{\eta}, \boldsymbol{\Theta}, \mathbf{f}^d, \mathbf{f}^u} \sum_{k=1}^{K_d} w_k^d f_k^d + \sum_{l=1}^{K_u} w_l^u f_l^u \\ \text{s.t.} \quad & f_k^d \leq \frac{S_k^d(\boldsymbol{\eta}, \boldsymbol{\Theta})}{p_k^d(\boldsymbol{\eta})}, f_l^u \leq \frac{S_l^u(\boldsymbol{\eta}, \boldsymbol{\Theta})}{p_l^u(\boldsymbol{\Theta})}, \\ & (2), (4), (20). \end{aligned} \quad (21)$$

Here $\mathbf{f}^\varepsilon \triangleq [f_1^\varepsilon \dots f_{K_\varepsilon}^\varepsilon] \in \mathbb{C}^{K_\varepsilon \times 1}$ are slack variables [22]. To approximate the non-convex constraints in (20) and (21) as convex, we substitute S_k^d and S_l^u from (14)-(15) and cross-multiply the terms p_k^d, p_l^u and f_k^d, f_l^u in (21). We also introduce slack variables $\boldsymbol{\Psi}^\varepsilon \triangleq [\Psi_1^\varepsilon, \dots, \Psi_{K_\varepsilon}^\varepsilon] \in \mathbb{C}^{K_\varepsilon \times 1}$, $\boldsymbol{\zeta}^\varepsilon \triangleq [\zeta_1^\varepsilon, \dots, \zeta_{K_\varepsilon}^\varepsilon] \in \mathbb{C}^{K_\varepsilon \times 1}$ and equivalently cast **P3** as follows [15]

$$\begin{aligned} \mathbf{P4} : \quad & \max_{\boldsymbol{\eta}, \boldsymbol{\Theta}, \mathbf{f}^d, \mathbf{f}^u, \boldsymbol{\Psi}^d, \boldsymbol{\Psi}^u, \boldsymbol{\zeta}^d, \boldsymbol{\zeta}^u} \sum_{k=1}^{K_d} w_k^d f_k^d + \sum_{l=1}^{K_u} w_l^u f_l^u \\ \text{s.t.} \quad & p_k^d \leq \frac{(\Psi_k^d)^2}{f_k^d}, p_l^u \leq \frac{(\Psi_l^u)^2}{f_l^u}, \end{aligned} \quad (22a)$$

$$(\Psi_k^d)^2 \leq \tau_f \log_2(1 + \zeta_k^d), (\Psi_l^u)^2 \leq \tau_f \log_2(1 + \zeta_l^u), \quad (22b)$$

$$\zeta_k^d \leq \frac{(\sum_{m \in \mathcal{M}_k^d} A_{mk}^d \sqrt{\eta_{mk}})^2}{\sum_{m=1}^M \sum_{q \in \kappa_{dm}} B_{kmq}^d \eta_{mq} + \sum_{l=1}^{K_u} D_{kl}^d \theta_l + 1}, \quad (22c)$$

$$\zeta_l^u \leq \frac{A_l^u \theta_l}{\sum_{q=1}^{K_u} B_{lq}^u \theta_q + \sum_{i=1}^M \sum_{k \in \kappa_{di}} D_{lik}^u \eta_{ik} + E_l^u \theta_l + F_l^u}, \quad (22d)$$

$$\log_2(1 + \zeta_k^d) \geq S_{ok}^d / \tau_f, \log_2(1 + \zeta_l^u) \geq S_{ol}^u / \tau_f, \quad (22e)$$

$$(2), (4).$$

We introduce the variable $c_{mk} \triangleq \sqrt{\eta_{mk}}$ and denote $\mathbf{C} \triangleq \{c_{mk}\} \in \mathbb{C}^{M \times K_d}$, to remove concave terms in (22c) arising due to $\sqrt{\eta_{mk}}$ and facilitate its conversion into a convex constraint. We

introduce additional slack variables $\lambda^\varepsilon \triangleq [\lambda_1^\varepsilon, \dots, \lambda_{K_\varepsilon}^\varepsilon] \in \mathbb{C}^{K_\varepsilon \times 1}$ to further simplify the non-convex constraints (22c)-(22d). We now cast **P4** equivalently as follows

$$\begin{aligned} \mathbf{P5} : \quad & \max_{\substack{C, \Theta, f^d, f^u \\ \Psi^d, \Psi^u, \zeta^d, \zeta^u, \lambda^d, \lambda^u}} \sum_{k=1}^{K_d} w_k^d f_k^d + \sum_{l=1}^{K_u} w_l^u f_l^u \\ \text{s.t.} \quad & \sum_{m=1}^M \sum_{q \in \kappa_{dm}} B_{kmq}^d c_{mq}^2 + \sum_{l=1}^{K_u} D_{kl}^d \theta_l + 1 \leq \frac{(\lambda_k^d)^2}{\zeta_k^d}, \end{aligned} \quad (23a)$$

$$\sum_{q=1}^{K_u} B_{lq}^u \theta_q + \sum_{i=1}^M \sum_{k \in \kappa_{di}} D_{lik}^u c_{ik}^2 + E_l^u \theta_l + F_l^u \leq \frac{(\lambda_l^u)^2}{\zeta_l^u}, \quad (23b)$$

$$\lambda_k^d \leq \sum_{m \in \mathcal{M}_k^d} A_{mk}^d c_{mk}, \quad (\lambda_l^u)^2 \leq A_l^u \theta_l, \quad (23c)$$

$$\lambda_k^d \geq 0, \tilde{b} \sum_{k \in \kappa_{dm}} \gamma_{mk}^d c_{mk}^2 \leq \frac{1}{N_t}, \quad c_{mk} \geq 0, \quad (23d)$$

(22a), (22b), (22e), (4).

We note that **P5** has all convex constraints except (22a) and (23a)-(23b). Since a first-order Taylor approximation is a global under-estimator of a convex function [22], we now linearize the right-hand side of these constraints. At the n th iteration, we substitute first-order Taylor approximate $\frac{f_1^2}{f_2} \geq 2 \frac{f_1^{(n)}}{f_2^{(n)}} f_1 - \frac{(f_1^{(n)})^2}{(f_2^{(n)})^2} f_2 \triangleq \Lambda^{(n)} \left(\frac{f_1^2}{f_2} \right)$ and use (16) to recast **P5** into a GCP:

$$\begin{aligned} \mathbf{P6} : \quad & \max_{\substack{C, \Theta, f^d, f^u \\ \Psi^d, \Psi^u, \zeta^d, \zeta^u, \lambda^d, \lambda^u}} \sum_{k=1}^{K_d} w_k^d f_k^d + \sum_{l=1}^{K_u} w_l^u f_l^u \\ \text{s.t.} \quad & \sum_{q=1}^{K_u} B_{lq}^u \theta_q + \sum_{i=1}^M \sum_{k \in \kappa_{di}} D_{lik}^u c_{ik}^2 + E_l^u \theta_l + F_l^u \leq \Lambda^{(n)} \left(\frac{(\lambda_l^u)^2}{\zeta_l^u} \right), \end{aligned} \quad (24a)$$

$$\sum_{m=1}^M \sum_{q \in \kappa_{dm}} B_{kmq}^d c_{mq}^2 + \sum_{l=1}^{K_u} D_{kl}^d \theta_l + 1 \leq \Lambda^{(n)} \left(\frac{(\lambda_k^d)^2}{\zeta_k^d} \right), \quad (24b)$$

$$P_{\text{fix}} + N_t \rho_d N_0 \sum_{m \in \mathcal{M}_k^d} \frac{1}{\alpha_m} \gamma_{mk}^d c_{mk}^2 + P_{\text{tc},k}^d \leq \Lambda^{(n)} \left(\frac{(\Psi_k^d)^2}{f_k^d} \right), \quad (24c)$$

$$P_{\text{fix}} + \rho_u N_0 \frac{1}{\alpha_l'} \theta_l + P_{\text{tc},l}^u \leq \Lambda^{(n)} \left(\frac{(\Psi_l^u)^2}{f_l^u} \right), \quad (24d)$$

(4), (22b), (22e), (23c), (23d).

We now first provide a centralized SCA procedure to solve **P6** in the second layer in Algorithm 2, and later propose a decentralized approach.

Algorithm 2: Centralized WSEE maximization algorithm

Input: i) Initialize power control coefficients $\{C, \Theta\}^{(1)}$ by allocating equal power to all downlink UEs being served and full power to all uplink UEs. Set $n = 1$.

ii) Initialize $\{f^d, f^u, \Psi^d, \Psi^u, \zeta^d, \zeta^u, \lambda^d, \lambda^u\}^{(1)}$ by replacing (23c), (24a)-(24b), (22b) and (24c)-(24d) by equality.

Output: Globally optimal power control coefficients $\{C, \Theta\}^*$

```

1 while  $\|r_{SCA}^{(n)}\| \leq \epsilon_{SCA}$  do
2   Solve P6 for the  $n$ th SCA iteration to obtain optimal variables,  $\{f^d, f^u, \Psi^d, \Psi^u, \zeta^d, \zeta^u, \lambda^d, \lambda^u, C, \Theta\}^{*,(n)}$ .
3   Assign the SCA iterates for the  $(n+1)$ th iteration,
    $\{f^d, f^u, \Psi^d, \Psi^u, \zeta^d, \zeta^u, \lambda^d, \lambda^u, C, \Theta\}^{(n+1)} = \{f^d, f^u, \Psi^d, \Psi^u, \zeta^d, \zeta^u, \lambda^d, \lambda^u, C, \Theta\}^{*,(n)}$ .

```

SCA Convergence Criterion: The residue after the n th SCA iteration, $r_{SCA}^{(n)}$, has a magnitude

$$\|r_{SCA}^{(n)}\| = \sqrt{\|C^{(n+1)} - C^{(n)}\|_F^2 + \|\Theta^{(n+1)} - \Theta^{(n)}\|^2}.$$

The SCA procedure converges when $\|r_{SCA}^{(n)}\| \leq \epsilon_{SCA}$, where ϵ_{SCA} is the convergence threshold.

Remark 1. (Convergence of centralized algorithm) At the n th SCA iteration, we use $V(n)$ to denote the GCP objective function value and $\mathcal{S}(n)$ as its feasible set of optimization variables. The set $\mathcal{S}(n)$ is, therefore, also feasible for the GCP formulated at the $(n+1)$ th iteration [24]. Algorithm 2, therefore, results in a non-decreasing sequence of the objective function values, i.e., $V(n+1) \geq V(n)$. The power constraints in (4), (23d) ensures that $V(n)$ is upper-bounded. This implies that Algorithm 2 always converges to a KKT point of **P2** due to [24, Prop. 3.2(ii)].

B. Decentralized ADMM approach

We now solve **P6** decentrally in the second layer using ADMM. The decentralized approach is well-suited for emerging architectures wherein the CPU consists of multiple distributed D-servers, connected via a central C-server [18], [19]. In ADMM, the centralized problem is decomposed into multiple sub-problems, each of which is solved by a D-server locally and independently. The C-server combines the local solutions to obtain a global solution. We observe that the constraints in (24a)-(24b) couple the power control coefficients of different uplink and downlink UEs. We next introduce global variables for the power control coefficients at the C-server, with local copies at the D-servers to decouple **P6** into sub-problems for each UE [21]. We observe that the constraints in **P6** for the downlink and uplink UEs can be divided between downlink and uplink D-servers, respectively. The D-servers solve sub-problems defined for each downlink and uplink UE. We first define local feasible sets at the n th SCA iteration for them, which are denoted as

$\mathcal{S}_k^{d,(n)}$ and $\mathcal{S}_l^{u,(n)}$, respectively. These sets are given as follows

$$\mathcal{S}_k^{d,(n)} = \left\{ f_k^d, \Psi_k^d, \zeta_k^d, \lambda_k^d, \tilde{\mathbf{C}}_k^d, \tilde{\Theta}_k^d \mid \tilde{b} \sum_{q \in \kappa_{dm}} \gamma_{mk}^d (\tilde{c}_{mq,k}^d)^2 \leq \frac{1}{N_t}, 0 \leq \tilde{\theta}_{l,k}^d \leq 1, \right. \quad (25a)$$

$$\lambda_k^d \leq \sum_{m \in \mathcal{M}_k^d} A_{mk}^d \tilde{c}_{mk,k}^d, \sum_{m=1}^M \sum_{q \in \kappa_{dm}} B_{kmq}^d (\tilde{c}_{mq,k}^d)^2 + \sum_{l=1}^{K_u} D_{kl}^d \tilde{\theta}_{l,k}^d + 1 \leq \Lambda^{(n)} \left(\frac{(\lambda_k^d)^2}{\zeta_k^d} \right), \quad (25b)$$

$$(\Psi_k^d)^2 \leq \tau_f \log_2(1 + \zeta_k^d), P_{\text{fix}} + N_t \rho_d N_0 \sum_{m \in \mathcal{M}_k^d} \frac{1}{\alpha_m} \gamma_{mk}^d (\tilde{c}_{mk,k}^d)^2 + P_{\text{tc},k}^d \leq \Lambda^{(n)} \left(\frac{(\Psi_k^d)^2}{f_k^d} \right), \quad (25c)$$

$$\tilde{c}_{mq,k}^d \geq 0 \forall q = 1 \text{ to } K_d, \lambda_k^d \geq 0, \log_2(1 + \zeta_k^d) \geq S_{ok}^d / \tau_f \}, \quad (25d)$$

$$\mathcal{S}_l^{u,(n)} = \left\{ f_l^u, \Psi_l^u, \zeta_l^u, \lambda_l^u, \tilde{\mathbf{C}}_l^u, \tilde{\Theta}_l^u \mid \tilde{b} \sum_{k \in \kappa_{dm}} \gamma_{mk}^d (\tilde{c}_{mk,l}^u)^2 \leq \frac{1}{N_t}, 0 \leq \tilde{\theta}_{q,l}^u \leq 1 \forall q = 1 \text{ to } K_u, \right. \quad (26a)$$

$$(\lambda_l^u)^2 \leq A_l^u \tilde{\theta}_{l,l}^u, \sum_{q=1}^{K_u} B_{lq}^u \tilde{\theta}_{q,l}^u + \sum_{i=1}^M \sum_{k \in \kappa_{di}} D_{lik}^u (\tilde{c}_{ik,l}^u)^2 + E_l^u \tilde{\theta}_{l,l}^u + F_l^u \leq \Lambda^{(n)} \left(\frac{(\lambda_l^u)^2}{\zeta_l^u} \right), \quad (26b)$$

$$(\Psi_l^u)^2 \leq \tau_f \log_2(1 + \zeta_l^u), P_{\text{fix}} + \rho_u N_0 \frac{1}{\alpha_l'} \tilde{\theta}_{l,l}^u + P_{\text{tc},l}^u \leq \Lambda^{(n)} \left(\frac{(\Psi_l^u)^2}{f_l^u} \right), \quad (26c)$$

$$\tilde{c}_{mk,l}^u \geq 0, \log_2(1 + \zeta_l^u) \geq S_{ol}^u / \tau_f \}. \quad (26d)$$

Here $\tilde{\mathbf{C}}_k^d, \tilde{\mathbf{C}}_l^u \in \mathbb{C}^{M \times K_d}$ and $\tilde{\Theta}_k^d, \tilde{\Theta}_l^u \in \mathbb{C}^{K_u \times 1}$ are local copies at the D-server of the corresponding global variables at the C-server, which are denoted as $\tilde{\mathbf{C}} \in \mathbb{C}^{M \times K_d}$ and $\tilde{\Theta} \in \mathbb{C}^{K_u \times 1}$, respectively, and represent the downlink and uplink power control coefficients, \mathbf{C} and Θ , in **P6**. We note that each D-server has its local power control variables and hence the constraints in (25)-(26), which are all convex, are independent for each D-server. This ensures that the sets $\mathcal{S}_k^{d,(n)}$ and $\mathcal{S}_l^{u,(n)}$ are convex. We define the sets of local variables for the D-servers corresponding to the downlink and uplink UEs as $\Omega_k^d \triangleq [\tilde{\mathbf{C}}_k^d, \tilde{\Theta}_k^d, f_k^d, \Psi_k^d, \lambda_k^d, \zeta_k^d]$ and $\Omega_l^u \triangleq [\tilde{\mathbf{C}}_l^u, \tilde{\Theta}_l^u, f_l^u, \Psi_l^u, \lambda_l^u, \zeta_l^u]$ respectively. We now reformulate **P6** as follows

$$\mathbf{P7} : \max_{\tilde{\mathbf{C}}, \tilde{\Theta}, \Omega_k^d, \Omega_l^u} \sum_{k=1}^{K_d} w_k^d f_k^d + \sum_{l=1}^{K_u} w_l^u f_l^u \quad (27a)$$

$$\text{s.t.} \quad \Omega_k^d \in \mathcal{S}_k^{d,(n)}, \Omega_l^u \in \mathcal{S}_l^{u,(n)},$$

$$\tilde{\mathbf{C}}_k^d = \tilde{\mathbf{C}}, \tilde{\mathbf{C}}_l^u = \tilde{\mathbf{C}}, \quad (27b)$$

$$\tilde{\Theta}_k^d = \tilde{\Theta}, \tilde{\Theta}_l^u = \tilde{\Theta}. \quad (27c)$$

To ensure that the global variables at the C-server have identical local copies maintained at the D-servers, we introduce the consensus constraints (27b)-(27c). The ADMM algorithm can now be readily applied to **P7** as it is in the global consensus form [23]. We denote $\varepsilon \triangleq \{d, u\}$ to denote downlink and uplink, respectively; $\phi \triangleq \{k, l\}$ to denote k th downlink UE and l th uplink UE, respectively. The sub-problems of the individual D-servers can now be written as follows

$$\mathbf{P7b} : \max_{\tilde{\mathbf{C}}, \tilde{\mathbf{\Theta}}, \mathbf{\Omega}_\phi^\varepsilon} w_\phi^\varepsilon f_\phi^\varepsilon \quad \text{s.t.} \quad \mathbf{\Omega}_\phi^\varepsilon \in \mathcal{S}_\phi^{\varepsilon, (n)}, \tilde{\mathbf{C}}_\phi^\varepsilon = \tilde{\mathbf{C}}, \tilde{\mathbf{\Theta}}_\phi^\varepsilon = \tilde{\mathbf{\Theta}}.$$

We now define auxiliary functions for the objective in **P7b** as follows

$$q_\phi^\varepsilon(\mathbf{\Omega}_\phi^\varepsilon) \triangleq \begin{cases} w_\phi^\varepsilon f_\phi^\varepsilon, & \mathbf{\Omega}_\phi^\varepsilon \in \mathcal{S}_\phi^{\varepsilon, (n)}, \\ -\infty, & \text{otherwise.} \end{cases} \quad (29)$$

We write, using (29), the augmented Lagrangian function for **P7** as

$$\begin{aligned} & \mathcal{L}^{(n)}(\tilde{\mathbf{C}}, \tilde{\mathbf{\Theta}}, \{\mathbf{\Omega}_k^d, \mathbf{\chi}_k^d, \mathbf{\xi}_k^d\}, \{\mathbf{\Omega}_l^u, \mathbf{\chi}_l^u, \mathbf{\xi}_l^u\}) \\ &= \sum_{k=1}^{K_d} \left(q_k^d(\mathbf{\Omega}_k^d) - \langle \mathbf{\chi}_k^d, \tilde{\mathbf{C}}_k^d - \tilde{\mathbf{C}} \rangle - \frac{\rho_C}{2} \|\tilde{\mathbf{C}}_k^d - \tilde{\mathbf{C}}\|_F^2 - \langle \mathbf{\xi}_k^d, \tilde{\mathbf{\Theta}}_k^d - \tilde{\mathbf{\Theta}} \rangle - \frac{\rho_\theta}{2} \|\tilde{\mathbf{\Theta}}_k^d - \tilde{\mathbf{\Theta}}\|^2 \right) \\ &+ \sum_{l=1}^{K_u} \left(q_l^u(\mathbf{\Omega}_l^u) - \langle \mathbf{\chi}_l^u, \tilde{\mathbf{C}}_l^u - \tilde{\mathbf{C}} \rangle - \frac{\rho_C}{2} \|\tilde{\mathbf{C}}_l^u - \tilde{\mathbf{C}}\|_F^2 - \langle \mathbf{\xi}_l^u, \tilde{\mathbf{\Theta}}_l^u - \tilde{\mathbf{\Theta}} \rangle - \frac{\rho_\theta}{2} \|\tilde{\mathbf{\Theta}}_l^u - \tilde{\mathbf{\Theta}}\|^2 \right), \quad (30) \end{aligned}$$

where $\rho_C, \rho_\theta > 0$ are the penalty parameters corresponding to the global variables $\tilde{\mathbf{C}}$ and $\tilde{\mathbf{\Theta}}$ respectively, and $\mathbf{\chi}_\phi^\varepsilon \in \mathbb{C}^{M \times K_d}, \mathbf{\xi}_\phi^\varepsilon \in \mathbb{C}^{K_u \times 1}$ are the Lagrangian variables associated with the equality constraints (27b) and (27c), respectively. The quadratic penalty terms are added to the objective to penalise equality constraints violations, and to enable the ADMM to converge by relaxing constraints of finiteness and strict convexity [23].

We note that the augmented Lagrangian in (30) is not decomposable in general for the problem formulation in **P7b** [22]. The auxiliary functions defined in (29) enable us to decompose it and formulate sub-problems for the D-servers. In ADMM method, the D-servers independently solve the sub-problems and update the local variables, which are collected by the C-server to update the global variables [23]. In the $(p+1)$ th iteration, following steps are executed in succession.

1) *Local computation*: The D-servers for each UE solve **P8** to update the local variables as

$$\begin{aligned} \mathbf{P8} : \mathbf{\Omega}_\phi^{\varepsilon, (p+1)} &= \arg \max_{\mathbf{\Omega}_\phi^\varepsilon} q_\phi^\varepsilon(\mathbf{\Omega}_\phi^\varepsilon) - \langle \mathbf{\chi}_\phi^{\varepsilon, (p)}, \tilde{\mathbf{C}}_\phi^\varepsilon - \tilde{\mathbf{C}}^{(p)} \rangle - \frac{\rho_C^{(p)}}{2} \|\tilde{\mathbf{C}}_\phi^\varepsilon - \tilde{\mathbf{C}}^{(p)}\|_F^2 \\ &- \langle \mathbf{\xi}_\phi^{\varepsilon, (p)}, \tilde{\mathbf{\Theta}}_\phi^\varepsilon - \tilde{\mathbf{\Theta}}^{(p)} \rangle - \frac{\rho_\theta^{(p)}}{2} \|\tilde{\mathbf{\Theta}}_\phi^\varepsilon - \tilde{\mathbf{\Theta}}^{(p)}\|^2. \quad (31) \end{aligned}$$

2) *Lagrangian multipliers update*: The D-servers now update the Lagrangian multipliers as

$$\chi_{\phi}^{\varepsilon,(p+1)} = \chi_{\phi}^{\varepsilon,(p)} + \rho_C^{(p)}(\tilde{C}_{\phi}^{\varepsilon,(p+1)} - \tilde{C}^{(p)}) \text{ and } \xi_{\phi}^{\varepsilon,(p+1)} = \xi_{\phi}^{\varepsilon,(p)} + \rho_{\theta}^{(p)}(\tilde{\Theta}_{\phi}^{\varepsilon,(p+1)} - \tilde{\Theta}^{(p)}). \quad (32)$$

3) *Global aggregation and computation*: The C-server now collects the updated local variables and Lagrangian multipliers from the D-servers and updates the global variables $\{\tilde{C}, \tilde{\Theta}\}$ as

$$\mathbf{P9} : \{\tilde{C}, \tilde{\Theta}\}^{(p+1)} = \arg \max_{\tilde{C}, \tilde{\Theta}} \mathcal{L}^{(n)} \left(\tilde{C}, \tilde{\Theta}, \{\Omega_k^d, \chi_k^d, \xi_k^d\}^{(p+1)}, \{\Omega_l^u, \chi_l^u, \xi_l^u\}^{(p+1)} \right).$$

Using (30) and maximizing w.r.t. each global variable, we obtain a closed form solution

$$\tilde{C}^{(p+1)} = \frac{1}{(K_u + K_d)} \left(\sum_{k=1}^{K_d} \left[\tilde{C}_k^{d,(p+1)} + \frac{1}{\rho_C^{(p)}} \chi_k^{d,(p+1)} \right] + \sum_{l=1}^{K_u} \left[\tilde{C}_l^{u,(p+1)} + \frac{1}{\rho_C^{(p)}} \chi_l^{u,(p+1)} \right] \right), \quad (33)$$

$$\tilde{\Theta}^{(p+1)} = \frac{1}{(K_u + K_d)} \left(\sum_{k=1}^{K_d} \left[\tilde{\Theta}_k^{d,(p+1)} + \frac{1}{\rho_{\theta}^{(p)}} \xi_k^{d,(p+1)} \right] + \sum_{l=1}^{K_u} \left[\tilde{\Theta}_l^{u,(p+1)} + \frac{1}{\rho_{\theta}^{(p)}} \xi_l^{u,(p+1)} \right] \right). \quad (34)$$

4) *Residue calculation and penalty parameter updates*: The C-server now calculates the squared magnitude of the primal and dual residuals, denoted as \mathbf{r}_{ADMM} and \mathbf{s}_{ADMM} respectively, as [23]

$$\|\mathbf{r}_{\text{ADMM}}^{(p+1)}\|_2^2 = \sum_{k=1}^{K_d} \left(\|\tilde{C}_k^d - \tilde{C}\|_F^2 + \|\tilde{\Theta}_k^d - \tilde{\Theta}\|_2^2 \right)^{(p+1)} + \sum_{l=1}^{K_u} \left(\|\tilde{C}_l^u - \tilde{C}\|_F^2 + \|\tilde{\Theta}_l^u - \tilde{\Theta}\|_2^2 \right)^{(p+1)}, \quad (35)$$

$$\|\mathbf{s}_{\text{ADMM}}^{(p+1)}\|_2^2 = (K_u + K_d) \left(\|\tilde{C}^{(p+1)} - \tilde{C}^{(p)}\|_F^2 + \|\tilde{\Theta}^{(p+1)} - \tilde{\Theta}^{(p)}\|_2^2 \right). \quad (36)$$

Using (35)-(36), the C-server updates penalty parameters for the $(p+1)$ th ADMM iteration as

$$\rho_{\{C,\theta\}}^{(p+1)} = \begin{cases} \rho_{\{C,\theta\}}^{(p)} \vartheta^{\text{incr}}, & \|r^{(p+1)}\|_2 > \mu \|s^{(p+1)}\|_2, \\ \rho_{\{C,\theta\}}^{(p)} / \vartheta^{\text{decr}}, & \|s^{(p+1)}\|_2 > \mu \|r^{(p+1)}\|_2, \\ \rho_{\{C,\theta\}}^{(p)}, & \text{otherwise.} \end{cases} \quad (37)$$

The parameters $\mu > 1, \vartheta^{\text{incr}} > 1, \vartheta^{\text{decr}} > 1$ are tuned to obtain good convergence [25].

Initialization for ADMM: At the $(n+1)$ th SCA iteration, we initialize the global variables at the C-server and their local copies at the D-servers with the SCA iteration variables as

$$\tilde{c}_{mk}^{(1)} = c_{mk}^{(n+1)}, \tilde{\theta}_l^{(1)} = \theta_l^{(n+1)}, \tilde{C}_k^{d,(1)} = \tilde{C}_l^{u,(1)} = \tilde{C}^{(1)}, \tilde{\Theta}_k^{d,(1)} = \tilde{\Theta}_l^{u,(1)} = \tilde{\Theta}^{(1)}. \quad (38)$$

ADMM Convergence Criterion: The ADMM can be said to have converged at iteration P if the primal residue is within a pre-determined tolerance limit ϵ_{ADMM} i.e., $\|r^{(P)}\|_2 \leq \epsilon_{\text{ADMM}}$.

The steps (31), (32), (33)-(34) and (37) are iterated until convergence, after which we obtain the locally optimal power control coefficients $\{\tilde{C}^*, \tilde{\Theta}^*\}$. We assign them to the iterates for the $(n+1)$ th SCA iteration, i.e., $\mathbf{C}^{(n+1)} = \tilde{C}^*, \mathbf{\Theta}^{(n+1)} = \tilde{\Theta}^*$. This concludes the n th SCA iteration.

The SCA is iterated till convergence. The steps for decentralized WSEE maximization using

SCA and ADMM are summarized in Algorithm 3.

Algorithm 3: Decentralized WSEE maximization algorithm using SCA and ADMM

Input: i) Initialize power control coefficients for SCA, $\{C, \Theta\}^{(1)}$ by allocating equal power to downlink UEs and maximum power to uplink UEs. Set $n = 1$. Initialize $\{f^d, f^u, \Psi^d, \Psi^u, \zeta^d, \zeta^u, \lambda^d, \lambda^u\}^{(1)}$ by replacing inequalities (23c), (24a)-(24b), (22b) and (24c)-(24d) by equality, in turn.

Output: Globally optimal power control coefficients $\{C, \Theta\}^*$

```

1 while  $\|r_{SCA}\| \leq \epsilon_{SCA}$  do
2   Set  $p = 1$ . Initialize global variables at C-server,  $\{\tilde{C}, \tilde{\Theta}\}^{(1)}$ , and local variables at D-servers,  $\Omega_\phi^{\epsilon, (1)}$ , using (38)
   and replacing inequalities (25b)-(25c) and (26b)-(26c) by equality.
3   while  $\|r_{ADMM}\| \leq \epsilon_{ADMM}$  do
4     Substitute  $\{C, \Theta, f^d, f^u, \Psi^d, \Psi^u, \zeta^d, \zeta^u, \lambda^d, \lambda^u\}^{(n)}$  in (25)-(26) to obtain feasible sets  $\mathcal{S}_\phi^{\epsilon, (n)}$ .
     Solve P8 at respective D-servers to update local variables  $\Omega_\phi^{\epsilon, (p+1)}$ .
     Solve (32) at respective D-servers to update Lagrangian multipliers  $\{\chi, \xi\}_\phi^{\epsilon, (p+1)}$ .
     At the C-server, collect the local variables  $\{\tilde{C}, \tilde{\Theta}\}_\phi^{\epsilon, (p+1)}$ , and the Lagrangian multipliers,  $\{\chi, \xi\}_\phi^{\epsilon, (p+1)}$ ,
     from the D-servers and solve (33)-(34) to update the global variables  $\tilde{C}^{(p+1)}, \tilde{\Theta}^{(p+1)}$ .
     At the C-server, update penalty parameters  $\rho_{C, \theta}^{(p+1)}$  according to (37) and broadcast them to all D-servers.
5   Update  $C^{(n+1)} = \tilde{C}^*, \Theta^{(n+1)} = \tilde{\Theta}^*$  and obtain  $\{f^d, f^u, \lambda^d, \lambda^u, \Psi^d, \Psi^u, \zeta^d, \zeta^u\}^{(n+1)}$  by replacing the
   inequalities (23c), (24a)-(24b), (22b) and (24c)-(24d) by equality.
6 return  $\{C, \Theta\}^*$ .

```

Remark 2. (Convergence of proposed decentralized algorithm) Algorithm 3 uses the iterative SCA technique with each SCA iteration involving the ADMM approach. The algorithm is guaranteed to converge if both SCA and ADMM converge. As discussed in Remark 1, the SCA iterative procedure surely converges to a KKT point of **P2**. For a given SCA iteration, the convergence of ADMM is guaranteed and investigated in detail in [23].

C. Computational complexity of centralized and decentralized algorithms

Before beginning this study, it is worth noting that both centralized Algorithm 2 and decentralized Algorithm 3 comprise of multiple steps that involve solving simple closed form expressions. These steps consume much lesser time than the ones which solve a GCP, typically using interior points methods [22]. We therefore compare the per-iteration complexity of centralized and decentralized algorithms by calculating the complexity of solving the respective GCPs.

- Algorithm 2 solves **P6** in step-1 of each SCA iteration, which has $4(K_u + K_d) + K_u + MK_d$ real variables and $6(K_u + K_d) + M + MK_d$ linear constraints. It has a worst-case computational complexity $\mathcal{O}\left((10(K_u + K_d) + K_u + M + 2MK_d)^{3/2}(4(K_u + K_d) + K_u + MK_d)^2\right)$ [26].
- Algorithm 3, in step-2 of each ADMM iteration, solves **P8** at the D-servers *in parallel* to update the local variables, therefore we need to analyse the computational complexity

at *any one of the* D-servers. Since the downlink has an additional constraint (second constraint in (25d)), we consider a downlink D-server for worst-case complexity analysis.

For a downlink D-server, **P8** has $MK_d + K_u + 4$ real variables and $MK_d + M + K_u + 6$ linear constraints. Therefore, it will have a worst-case computational complexity of $\mathcal{O}\left((2MK_d + M + 2K_u + 10)^{3/2} (MK_d + K_u + 4)^2\right)$ [26].

We consider equal number of uplink and downlink UEs, i.e., $K_d = K_u = K/2$, for this analysis. We can observe that when the number of UEs, K , is taken to be large, Algorithm 3 will have a much lower computational complexity than Algorithm 2.

V. SIMULATION RESULTS

We now numerically investigate the WSEE of a FD CF mMIMO system with limited capacity fronthaul links using the proposed two-layer decentralized optimization approach. We assume a realistic system model wherein M APs, K_d downlink UEs and K_u uplink UEs are scattered in a square of size D km \times D km. To avoid the boundary effects [2], we wrap the APs and UEs around the edges [5]. We denote $\varepsilon \triangleq \{d, u\}$ to denote downlink and uplink, respectively; $\phi \triangleq \{k, l\}$ to denote k th downlink UE and l th uplink UE, respectively. The large-scale fading coefficients, $\beta_{m\phi}^\varepsilon$, are modeled as [11]

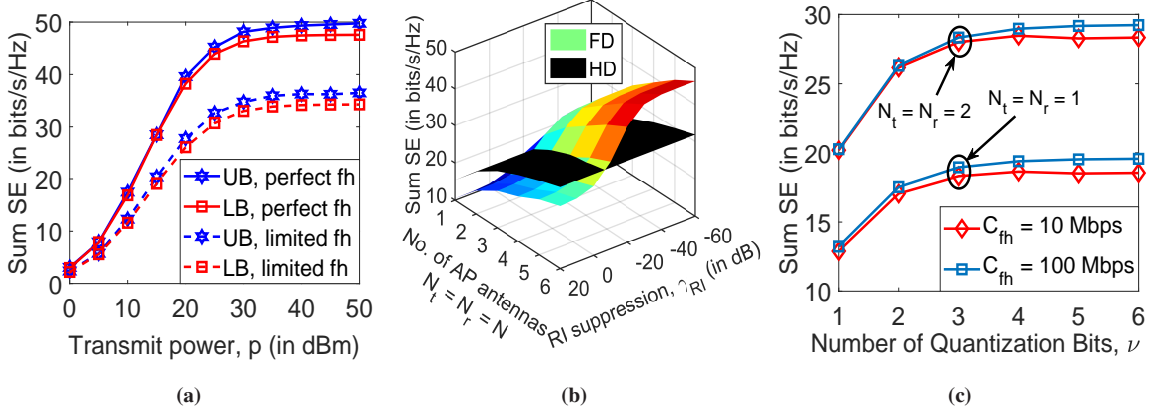
$$\beta_{m\phi}^\varepsilon = 10^{\frac{\text{PL}_{m\phi}^\varepsilon}{10}} 10^{\frac{\sigma_{\text{sd}} z_{m\phi}^\varepsilon}{10}}. \quad (39)$$

Here $10^{\frac{\sigma_{\text{sd}} z_{m\phi}^\varepsilon}{10}}$ is the log-normal shadowing factor having a standard deviation σ_{sd} (in dB) and $z_{m\phi}^\varepsilon$ follows a two-components correlated model [2]. The path loss $\text{PL}_{m\phi}^\varepsilon$ (in dB) follows a three-slope model [2], [5]. We, similar to [5], model the large-scale fading coefficients for the inter-AP RI channels, i.e., $\beta_{\text{RI},mi}$, $\forall i \neq m$, as in (39), and assume that the large-scale fading for the intra-AP RI channels, which experience no shadowing, are modeled as $\beta_{\text{RI},mm} = 10^{\frac{\text{PL}_{\text{RI}}(\text{dB})}{10}}$. The inter-UE large scale fading coefficients, $\tilde{\beta}_{kl}$, are also modeled similar to (39). We consider, for brevity, same number of quantization bits, ν , and same capacity, C_{fh} , on all fronthaul links. We, henceforth, denote the transmit powers on the downlink and uplink as p_d ($= \rho_d N_0$) and p_u ($= \rho_u N_0$), respectively, and the pilot transmit power as p_t ($= \rho_t N_0$). Similar to [2], [5], [8], [11], [12], we fix the values for the system model and power consumption model parameters, unless mentioned otherwise, as given in Table I.

Validation of achievable SE expressions: We consider an FD CF mMIMO system with $M = 32$ APs, each having $N_t = N_r = N = 2$ transmit and receive antennas, and $K_d = K_u = K/2 = 10$ uplink and downlink UEs and consider equal transmit power for uplink and

Table I: Full-Duplex Cell-Free mMIMO system model and power consumption model parameters

Parameter	Value	Parameter	Value
D, τ_c, T_c	1 km, 200, 1 ms	σ_{sd}, B	2 dB, 20 Mhz
Fronthaul parameters ν, C_{fh}	2, 100 Mbps	γ_{RI}, PL_{RI} (in dB)	-20, -81.1846
$P_{ft}, P_{0,m}, P_{tc,m} = P_{tc,k}^d = P_{tc,l}^u, p_t$ (in W)	10, 0.825, 0.2, 0.2	$N_0, \alpha_m = \alpha_l'$	-121.4 dB, 0.4

**Fig. 2:** a) Sum SE (analytical LB and ergodic UB) vs Transmit power, with $M = 32, N_t = N_r = 2, K_d = K_u = 10$; b) Sum SE vs RI suppression levels and (c) Sum SE vs Number of quantization bits, with $M = 32, K_d = K_u = 10, p = 30$ dBm.

downlink data transmission, i.e., $p_d = p_u = p$. We verify in Fig. 2a the tightness of the SE lower bound derived in (14)-(15), labeled as LB, by comparing it with the numerically obtained ergodic SE in (10), labeled as upper-bound (UB) as it requires instantaneous CSI. The large-scale fading coefficients are set to unity, i.e., $\beta_{mk}^d = \beta_{ml}^u = 1, \forall k \in \kappa_{dm}, l \in \kappa_{um}$. We, similar to [2], [11], allocate equal power to all downlink UEs and full power to all uplink UEs, i.e., $\eta_{mk} = (bN_t (\sum_{k \in \kappa_{dm}} \gamma_{mk}^d))^{-1}, \forall k \in \kappa_{dm}$ and $\theta_l = 1$. We consider two fronthaul cases: i) perfect high-capacity with $\tilde{a} = \tilde{b} = 1$, and ii) limited capacity, with $\nu = 2$ quantization bits and capacity $C_{fh} = 10$ Mbps. We see that the derived lower bound is tight for perfect- and limited-capacity fronthauls. With limited fronthaul, the sum SE significantly drops, as quantization attenuates and distorts the signal and limits the number of UEs that each AP can serve (see (9)).

Sum SE - effect of system parameters: We next investigate the sum SE with important system parameters. We consider an FD CF mMIMO system with $M = 32$ APs, $K_u = K_d = K/2 = 10$ uplink and downlink UEs and with transmit power $p_u = p_d = p = 30$ dBm.

We compare in Fig. 2b the FD CF mMIMO system with varying levels of RI suppression factor γ_{RI} and an equivalent HD system which serves uplink and downlink UEs in time-division duplex mode by using all AP antennas. For the HD system, we i) set $\gamma_{RI} = 0$ and inter-UE

channel gains $\tilde{\beta}_{kl} = 0$; ii) use all AP antennas, i.e., $N = (N_t + N_r)$, during uplink and downlink transmission; and iii) multiply sum SE with a factor of $(1/2)$. We consider limited fronthaul with $\nu = 2$ quantization bits and capacity $C_{\text{fh}} = 10$ Mbps. We see that the FD system has a significantly higher sum SE than an equivalent HD system, provided the RI suppression is good ($\gamma_{\text{RI}} \leq -10$ dB). The sum SE does not double, even with significant RI suppression $\gamma_{\text{RI}} \leq -40$ dB. This is due to the UDI experienced by the downlink UEs in a FD CF mMIMO system as shown in Fig. 1, which cannot be mitigated by RI suppression at the APs.

We plot in Fig. 2c the sum SE by varying the number of fronthaul quantization bits ν . We consider $N_t = N_r = \{1, 2\}$ transmit and receive antennas on each AP and fronthaul with $C_{\text{fh}} = 10$ and 100 Mbps. We observe that in both cases, the sum SE increases with increase in ν initially and then saturates. Increasing ν reduces the quantization distortion and attenuation, thereby improving the sum SE. This effect, however, saturates as after a limit most of the information is retrieved. We observe that reducing the fronthaul capacity from $C_{\text{fh}} = 100$ Mbps to $C_{\text{fh}} = 10$ Mbps reduces the sum SE slightly, as the procedure outlined in Section II-D *fairly* retains the AP-UE links with the highest channel gains and helps maintain the sum SE.

WSEE metric - influence of weights: We now demonstrate that the WSEE metric can accommodate the heterogeneous EE requirements of both uplink and downlink UEs. For this study, we consider a particular realization of a FD CF mMIMO system with a transmit power $p_d = p_u = 30$ dBm, $M = 32$ APs, $K_d = K_u = K/2 = 2$ uplink and downlink UEs and $N_t = N_r = N = 2$ transmit and receive antennas on each AP, with QoS constraints $S_{ok} = S_{ol} = 0.1$ bits/s/Hz. We plot the individual EEs of the uplink (UL) and downlink (DL) UEs versus the SCA iteration index for centralized WSEE maximization, using Algorithm 2, for two different combinations of UE weights. Weights w_1 and w_2 are associated with DL UE 1 and DL UE 2, while weights w_3 and w_4 are associated with UL UE 1 and UL UE 2, respectively.

We plot in Fig. 3a and Fig. 3b the individual EEs of UL and DL UEs, with: i) equal weights ($w_1 = w_2 = w_3 = w_4 = 0.25$), and ii) $w_1 = 0.08$, $w_2 = 0.02$, $w_3 = 0.5$, $w_4 = 0.4$, respectively. In Fig. 3a, with equal weights, UEs attain an EE depending on their relative channel conditions, which clearly indicates that in terms of channel conditions, DL UE 2 \gg DL UE 1 $>$ UL UE 2 $>$ UL UE 1. In Fig. 3b, the weights are chosen in an order which is opposite to the channel conditions. The EEs of the UL UEs dominate the EE of DL UE 1, while reversing their relative order. DL UE 2, with excellent channel, still attains a high EE, although lower than in Fig. 3a.

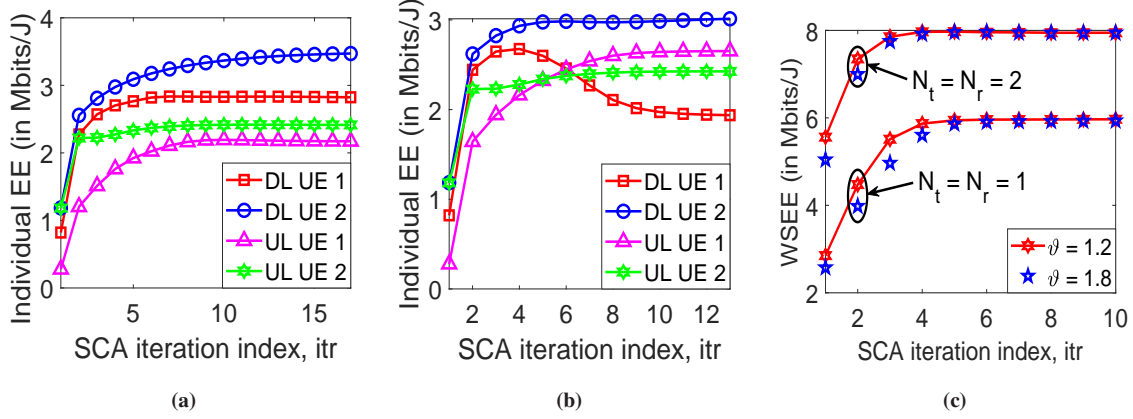


Fig. 3: Effect of UE priorities on individual EEs with $M = 32$, $K_d = K_u = 2$, $N_t = N_r = 2$ and $S_{ok} = S_{ol} = 0.1$ bits/s/Hz: (a) $w_1 = w_2 = w_3 = w_4 = 0.25$, (b) $w_1 = 0.08, w_2 = 0.02, w_3 = 0.5, w_4 = 0.4$; c) Convergence of decentralized algorithm.

Convergence of decentralized ADMM algorithm: We plot in Fig. 3c the WSEE obtained using decentralized Algorithm 3 with SCA iteration index. We consider $M = 10$ APs, $K_u = K_d = K/2 = 2$ uplink and downlink UEs and $N_t = N_r = \{1, 2\}$ transmit and receive antennas on each AP at transmit power $p_d = p_u = p = 30$ dBm. We assume the following: i) penalty parameters $\rho_C = \rho_\theta = 0.1$; ii) penalty parameter update threshold factor $\mu = 10$; iii) ADMM convergence threshold $\epsilon_{\text{ADMM}} = 0.01$; and iv) SCA convergence threshold $\epsilon_{\text{SCA}} = 0.001$. We consider two values of the penalty update parameter: $\vartheta = \{1.2, 1.8\}$. We note that the algorithm in both cases converges marginally quicker with $\vartheta = 1.2$. A smaller penalty update parameter is therefore beneficial as then changes in the penalty parameters are not too abrupt, and a bad ADMM iteration which causes the primal and dual residues to diverge is, consequently, not overly responded to [25]. We therefore fix $\vartheta = 1.2$ for the rest of the simulations.

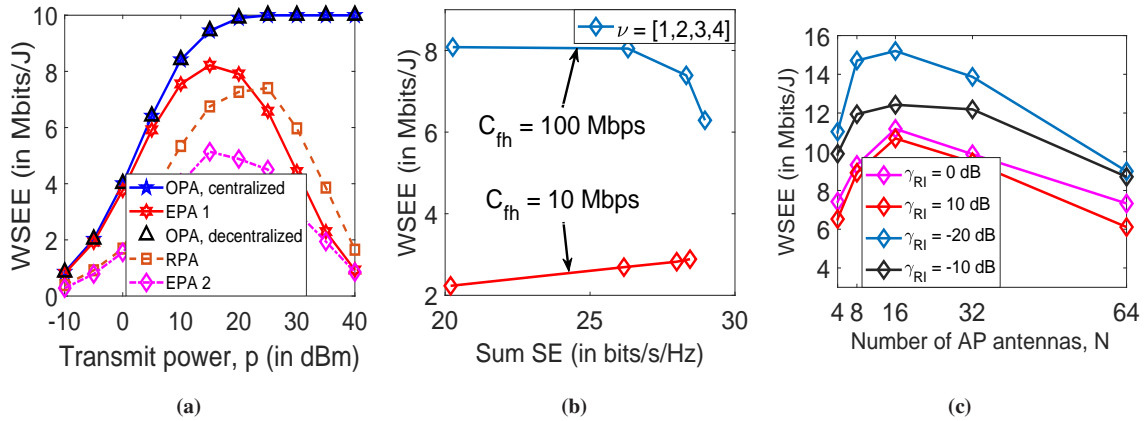


Fig. 4: WSEE vs (a) Maximum transmit power and (b) Sum SE by varying $\nu = 1$ to 4, with $M = 32$, $K_d = K_u = 10$, $N_t = N_r = 2$ and $S_{ok} = S_{ol} = 0.1$ bits/s/Hz; (c) Number of AP antennas, with $K_d = K_u = 10$ and $S_{ok} = S_{ol} = 0.1$ bits/s/Hz

WSEE maximization - optimal system parameters: We now study WSEE variation with important system model parameters and thereby obtain crucial insights into designing an energy-

efficient FD CF mMIMO system. We consider $M = 32$ APs, $N_t = N_r = N = 2$ transmit and receive antennas on each AP, $K_u = K_d = K/2 = 10$ downlink and uplink UEs and QoS constraints $S_{ok} = S_{ol} = 0.1$ bits/s/Hz, unless mentioned otherwise.

We plot in Fig. 4a the WSEE versus transmit power p , which is taken to be equal for downlink and uplink, i.e., $p_d = p_u = p$. We consider centralized optimal power allocation (OPA) in Algorithm 2, labeled as “OPA, centralized”, and decentralized approach in Algorithm 3, labeled as “OPA, decentralized”, and compare them with three sub-optimal power allocation schemes: i) equal power allocation of type 1, labeled as “EPA 1”, where $\eta_{mk} = (bN_t (\sum_{k \in \kappa_{dm}} \gamma_{mk}^d))^{-1}$, $\forall k \in \kappa_{dm}$ and $\theta_l = 1$ [11], [12], ii) equal power allocation of type 2, labeled as “EPA 2”, where $\eta_{mk} = (bN_t K_{dm} \gamma_{mk}^d)^{-1}$, $\forall k \in \kappa_{dm}$ and $\theta_l = 1$ [11], and iii) random power allocation, labeled as “RPA”, where power control coefficients are chosen randomly from a uniform distribution between 0 and the “EPA 1” value. We note that existing literature has not yet optimized the WSEE metric for CF mMIMO systems, and hence we can only compare with above sub-optimal schemes. We note that both decentralized and centralized approaches far outperform the baseline schemes. We note that the decentralized ADMM approach, with lower computational complexity, has same WSEE as the centralized one.

We next quantify in Fig. 4b the joint variation of WSEE and the sum SE, with the number of quantization bits, ν , in the fronthaul links. We note that the WSEE is obtained using decentralized Algorithm 3. We consider transmit power $p_d = p_u = p = 30$ dBm and take two different cases: i) high fronthaul capacity, $C_{fh} = 100$ Mbps, which is sufficiently high to support all the UEs, and ii) limited fronthaul capacity, $C_{fh} = 10$ Mbps, which limits the number of UEs a single AP can serve. We observe that for $C_{fh} = 100$ Mbps, the WSEE falls with increase in ν , even though the corresponding sum SE increases. For $C_{fh} = 10$ Mbps, the sum SE and the WSEE simultaneously increase with increase in ν . To explain this behaviour, we note from Fig. 2c that increasing ν improves the sum SE for both the cases. For $C_{fh} = 100$ Mbps, the APs serve all the UEs, i.e., $K_{dm} = K_d$ and $K_{um} = K_u$, so increasing ν linearly increases the fronthaul data rate, R_{fh} (see (7)). This, as seen from (17), increases the traffic-dependent fronthaul power consumption. Using lower number (1-2) of quantization bits is therefore more energy-efficient, as it provides sufficiently good SE with a low energy consumption. However, for $C_{fh} = 10$ Mbps, K_{um} and K_{dm} have an upper limit, given by (9), which is inversely related to ν . The product, $\nu(K_{um} + K_{dm})$, remains nearly constant for all values of ν . Thus, R_{fh} (see (7)) doesn't increase

with increase in ν and remains close to the capacity, C_{fh} . The traffic-dependent fronthaul power consumption, given in (17), hence, remains close to P_{ft} . A higher number (3-4) of quantization bits therefore provides a higher sum SE and hence, also maximizes the WSEE.

We now numerically investigate in Fig. 4c the WSEE dependence on the number of transmit and receive antennas on each AP ($N_t = N_r = N$) for different values of RI suppression factor, γ_{RI} . We consider transmit power $p_d = p_u = p = 30$ dBm and fix the total number of AP antennas as $MN = 128$. Increasing the number of APs M , increases the sum SE and the fronthaul power consumption. Therefore, there exists a trade-off here, and we use the flexibility of having multiple antennas at the APs to explore different system designs for the same total number of AP antennas. We observe that among all cases, $N = 16, M = 8$ has the best WSEE. We also observe that with improved RI suppression, i.e., lower value of γ_{RI} , the WSEE increases. This is due to reduced RI in the uplink which, as shown in Fig. 2b, improves the sum SE.

VI. CONCLUSION

We derived the achievable SE expressions for a FD CF mMIMO wireless system with optimal uniform fronthaul quantization. Using a *two-layered* approach, we optimized the non-convex WSEE using SCA framework which in each iteration solves a GCP either centrally or decentrally using ADMM. We also numerically investigated how WSEE incorporates EE requirements of different UEs. We demonstrated the convergence of decentralized algorithm both analytically and numerically. We showed that it achieves the same WSEE as the centralized approach with a much reduced computational complexity. Finally, we numerically investigated the WSEE dependence on various system parameters which gives important insights to design energy-efficient systems.

APPENDIX A

We follow the optimal uniform quantization model as considered in [8], [12]. Using Bussgang decomposition [27], the quantization function $\mathcal{Q}(x) = \tilde{a}x + \sqrt{p_x}\tilde{\zeta}_d$, where $\tilde{a} = \frac{1}{p_x} \int_{\mathcal{X}} xh(x)f_X(x)dx$, $\tilde{b} = \frac{1}{p_x} \int_{\mathcal{X}} h^2(x)f_X(x)dx$ and $\tilde{\zeta}_d$ is the normalized distortion whose power is given as $\mathbb{E}\{\tilde{\zeta}_d^2\} = \tilde{b} - \tilde{a}^2$. Here $h(x)$ is the mid-rise uniform quantizer with $L = 2^\nu$ quantization levels rising in steps of size $\tilde{\Delta}$ and ν is the number of quantization bits. The signal-to-distortion ratio (SDR) is

$$\text{SDR} = \frac{\mathbb{E}\{(\tilde{a}x)^2\}}{p_x \mathbb{E}\{\tilde{\zeta}_d^2\}} = \frac{\tilde{a}^2}{\tilde{b} - \tilde{a}^2}. \quad (40)$$

The optimal step-size $\tilde{\Delta}_{\text{opt}}$ is the one which maximizes the SDR. The optimal values of \tilde{a} and \tilde{b} , are calculated using (40), and given in Table II [8].

APPENDIX B

We now derive the achievable SE expression for the l th uplink UE in (15). We know, from Section II-B, that $\mathbf{g}_{ml}^u = \hat{\mathbf{g}}_{ml}^u + \mathbf{e}_{ml}^u$, where $\hat{\mathbf{g}}_{ml}^u$ and \mathbf{e}_{ml}^u are independent and $\mathbb{E}\{\|\hat{\mathbf{g}}_{ml}^u\|^2\} = N_r \gamma_{ml}^u$.

Table II: Optimal Uniform Quantization Parameters

ν	$\tilde{\Delta}_{\text{opt}}$	$\mathbb{E}\{\tilde{\zeta}_d^2\} = \tilde{b} - \tilde{a}^2$	\tilde{a}	ν	$\tilde{\Delta}_{\text{opt}}$	$\mathbb{E}\{\tilde{\zeta}_d^2\} = \tilde{b} - \tilde{a}^2$	\tilde{a}
1	1.596	0.2313	0.6366	5	0.1881	0.003482	0.996505
2	0.9957	0.10472	0.88115	6	0.1041	0.0010389	0.99896
3	0.586	0.036037	0.96256	7	0.0568	0.0003042	0.99969
4	0.3352	0.011409	0.98845	8	0.0307	0.0000876	0.999912

We can express the desired signal for the l th uplink UE as

$$\mathbb{E}\{|\text{DS}_l^u|^2\} = \mathbb{E}\left\{\left|\tilde{a} \sum_{m \in \mathcal{M}_l^u} \sqrt{\rho_u} \mathbb{E}\{\sqrt{\theta_l}(\hat{\mathbf{g}}_{ml}^u)^H (\hat{\mathbf{g}}_{ml}^u + \mathbf{e}_{ml}^u) s_l^u\}\right|^2\right\} = \tilde{a}^2 N_r^2 \rho_u \theta_l \left(\sum_{m \in \mathcal{M}_l^u} \gamma_{ml}^u\right)^2. \quad (41)$$

We express the beamforming uncertainty for the l th uplink UE as

$$\begin{aligned} \mathbb{E}\{|\text{BU}_l^u|^2\} &= \tilde{a}^2 \rho_u \sum_{m \in \mathcal{M}_l^u} \mathbb{E}\{\|(\sqrt{\theta_l}(\hat{\mathbf{g}}_{ml}^u)^H \mathbf{g}_{ml}^u s_l^u - \mathbb{E}\{\sqrt{\theta_l}(\hat{\mathbf{g}}_{ml}^u)^H \mathbf{g}_{ml}^u s_l^u\})\|^2\} \\ &\stackrel{(a)}{=} \tilde{a}^2 \rho_u \sum_{m \in \mathcal{M}_l^u} (\mathbb{E}\{\|\hat{\mathbf{g}}_{ml}^u\|^4\} + \mathbb{E}\{|\hat{\mathbf{g}}_{ml}^u{}^H \mathbf{e}_{ml}^u|^2\} - N_r^2 (\gamma_{ml}^u)^2) \theta_l \\ &\stackrel{(b)}{=} \tilde{a}^2 \rho_u \sum_{m \in \mathcal{M}_l^u} (N_r(N_r+1)(\gamma_{ml}^u)^2 + N_r \gamma_{ml}^u (\beta_{ml}^u - \gamma_{ml}^u) - N_r^2 (\gamma_{ml}^u)^2) \theta_l = \tilde{a}^2 \rho_u N_r \sum_{m \in \mathcal{M}_l^u} \gamma_{ml}^u \beta_{ml}^u \theta_l. \end{aligned} \quad (42)$$

Equality (a) is obtained by i) using $\mathbb{E}\{|s_l^u|^2\} = 1$; ii) substituting $\mathbf{g}_{ml}^u = \hat{\mathbf{g}}_{ml}^u + \mathbf{e}_{ml}^u$; and iii) using the fact that \mathbf{e}_{ml}^u and $\hat{\mathbf{g}}_{ml}^u$ are zero-mean and uncorrelated; iv) using $\mathbb{E}\{|\hat{\mathbf{g}}_{ml}^u|^2\} = N_r \gamma_{ml}^u$. Equality (b) is obtained using the results $\mathbb{E}\{\|\hat{\mathbf{g}}_{ml}^u\|^4\} = N_r(N_r+1)(\gamma_{ml}^u)^2$ [28] and $\mathbb{E}\{\|\mathbf{e}_{ml}^u\|^2\} = (\beta_{ml}^u - \gamma_{ml}^u)$. We simplify the multi-UE interference for the l th uplink UE as

$$\begin{aligned} \mathbb{E}\{|\text{MUI}_l^u|^2\} &= \tilde{a}^2 \rho_u \sum_{m \in \mathcal{M}_l^u} \sum_{q=1, q \neq l}^{K_u} \mathbb{E}\{|\sqrt{\theta_q}(\hat{\mathbf{g}}_{ml}^u)^H \mathbf{g}_{mq}^u s_q^u - \mathbb{E}\{\sqrt{\theta_q}(\hat{\mathbf{g}}_{ml}^u)^H \mathbf{g}_{mq}^u s_q^u\}|^2\} \\ &= \tilde{a}^2 \rho_u \sum_{m \in \mathcal{M}_l^u} \sum_{q=1, q \neq l}^{K_u} \mathbb{E}\{|\hat{\mathbf{g}}_{ml}^u{}^H \mathbf{g}_{mq}^u|^2\} - (\mathbb{E}\{|\hat{\mathbf{g}}_{ml}^u{}^H \mathbf{g}_{mq}^u\}|)^2 \theta_q \stackrel{(a)}{=} \tilde{a}^2 \rho_u N_r \sum_{m \in \mathcal{M}_l^u} \sum_{q=1, q \neq l}^{K_u} \gamma_{ml}^u \beta_{mq}^u \theta_q. \end{aligned} \quad (43)$$

Equality (a) is obtained by using these facts: i) $\hat{\mathbf{g}}_{ml}^u$, \mathbf{g}_{mq}^u are mutually independent; and

$$\text{ii) } \mathbb{E}\{|\hat{\mathbf{g}}_{ml}^u{}^H \mathbf{g}_{mq}^u|^2\} = \mathbb{E}\{(\mathbf{g}_{mq}^u)^H \mathbb{E}\{(\hat{\mathbf{g}}_{ml}^u)(\hat{\mathbf{g}}_{ml}^u)^H\} \mathbf{g}_{mq}^u\} = \gamma_{ml}^u \mathbb{E}\{(\mathbf{g}_{mq}^u)^H \mathbf{g}_{mq}^u\} = \gamma_{ml}^u \mathbb{E}\{|\mathbf{g}_{mq}^u|^2\} = N_r \gamma_{ml}^u \beta_{mq}^u.$$

We now simplify $\mathbb{E}\{|\text{RI}_l^u|^2\} = \tilde{a}^2 \rho_d \sum_{m \in \mathcal{M}_l^u} \sum_{i=1}^M \sum_{k \in \kappa_{di}} \mathbb{E}\{|\hat{\mathbf{g}}_{ml}^u{}^H \mathbf{H}_{mi}(\hat{\mathbf{g}}_{ik}^d)^*|^2\}(\tilde{a}^2 + b - \tilde{a}^2)\eta_{ik}$

$$\stackrel{(a)}{=} \tilde{a}^2 \tilde{b} N_r N_t \rho_d \sum_{m \in \mathcal{M}_l^u} \sum_{i=1}^M \sum_{k \in \kappa_{di}} \gamma_{ml}^u \gamma_{ik}^d \beta_{\text{RI},mi} \gamma_{\text{RI}} \eta_{ik}. \quad (44)$$

Equality (a) is because: i) channels $\hat{\mathbf{g}}_{ml}^u$, \mathbf{H}_{mi} and $\hat{\mathbf{g}}_{mk}^d$ are mutually independent; ii) $\gamma_{\text{RI},mi} = \beta_{\text{RI},mi} \gamma_{\text{RI}}$, $i = 1$ to M ; and iii) the result

$$\begin{aligned} \mathbb{E}\{|\hat{\mathbf{g}}_{ml}^u{}^H \mathbf{H}_{mi}(\hat{\mathbf{g}}_{ik}^d)^*|^2\} &= \mathbb{E}\{(\hat{\mathbf{g}}_{ik}^d)^T \mathbb{E}\{\mathbf{H}_{mi}^H \mathbb{E}\{(\hat{\mathbf{g}}_{ml}^u)(\hat{\mathbf{g}}_{ml}^u)^H\} \mathbf{H}_{mi}\}(\hat{\mathbf{g}}_{ik}^d)^*\} = \gamma_{ml}^u \mathbb{E}\{(\hat{\mathbf{g}}_{ik}^d)^T \mathbb{E}\{\mathbf{H}_{mi}^H \mathbf{H}_{mi}\}(\hat{\mathbf{g}}_{ik}^d)^*\} \\ &= N_r \gamma_{ml}^u \beta_{\text{RI},mi} \gamma_{\text{RI}} \mathbb{E}\{(\hat{\mathbf{g}}_{ik}^d)^T (\hat{\mathbf{g}}_{ik}^d)^*\} = N_r N_t \gamma_{ml}^u \gamma_k^d \beta_{\text{RI},mi} \gamma_{\text{RI}}. \end{aligned} \quad (45)$$

We next obtain the noise power for the l th uplink UE as

$$\mathbb{E}\{|N_l^u|^2\} = \tilde{a}^2 \sum_{m \in \mathcal{M}_l^u} \mathbb{E}\{|(\hat{\mathbf{g}}_{ml}^u)^H \mathbf{w}_m^u|^2\} \stackrel{(a)}{=} \tilde{a}^2 N_r \sum_{m \in \mathcal{M}_l^u} \gamma_{ml}^u. \quad (46)$$

Equality (a) is because: i) estimated channel $\hat{\mathbf{g}}_{ml}^u$ and receiver noise \mathbf{w}_m^u are uncorrelated, and

$$\text{ii) } \mathbb{E}\{|(\hat{\mathbf{g}}_{ml}^u)^H \mathbf{w}_m^u|^2\} = \mathbb{E}\{(\mathbf{w}_m^u)^H \mathbb{E}\{\hat{\mathbf{g}}_{ml}^u (\hat{\mathbf{g}}_{ml}^u)^H\} \mathbf{w}_m^u\} = \gamma_{ml}^u \mathbb{E}\{(\mathbf{w}_m^u)^H \mathbf{w}_m^u\} = N_r \gamma_{ml}^u. \quad (47)$$

Total quantization distortion for the l th uplink UE is given as

$$\begin{aligned} \mathbb{E}\{|\text{TQD}_l^u|^2\} &\approx (\tilde{b} - \tilde{a}^2) \sum_{m \in \mathcal{M}_l^u} \mathbb{E}\{|\hat{\mathbf{g}}_{ml}^u{}^H \mathbf{y}_m|^2\}, \text{ where} \\ \mathbb{E}\{|\hat{\mathbf{g}}_{ml}^u{}^H \mathbf{y}_m|^2\} &= \rho_u \theta_l \mathbb{E}\{|\hat{\mathbf{g}}_{ml}^u{}^H \mathbf{g}_{ml}^u|^2\} + \rho_d \sum_{i=1}^M \sum_{k \in \kappa_{di}} \mathbb{E}\{|\hat{\mathbf{g}}_{ml}^u{}^H \mathbf{H}_{mi} (\hat{\mathbf{g}}_{ik}^d)^*|^2\} \tilde{b} \eta_{ik} + \mathbb{E}\{|\hat{\mathbf{g}}_{ml}^u{}^H \mathbf{w}_m^u|^2\} \\ &\stackrel{(a)}{=} \rho_u \theta_l (\mathbb{E}\{\|\hat{\mathbf{g}}_{ml}^u\|^2 + (\hat{\mathbf{g}}_{ml}^u)^H \mathbf{e}_{ml}^u\}^2) + \tilde{b} N_r N_t \rho_d \sum_{i=1}^M \sum_{k \in \kappa_{di}} \gamma_{ml}^u \gamma_{ik}^d \beta_{\text{RI},mi} \gamma_{\text{RI}} \eta_{ik} + N_r \gamma_{ml}^u \\ &\stackrel{(b)}{=} N_r^2 \rho_u (\gamma_{ml}^u)^2 \theta_l + \rho_u N_r \gamma_{ml}^u \sum_{q=1}^{K_u} \beta_{mq}^u \theta_q + \tilde{b} N_r N_t \rho_d \sum_{i=1}^M \sum_{k \in \kappa_{di}} \gamma_{ml}^u \gamma_{ik}^d \beta_{\text{RI},mi} \gamma_{\text{RI}} \eta_{ik} + N_r \gamma_{ml}^u. \end{aligned} \quad (48)$$

Equality (a) follows from i) $\mathbb{E}\{|\zeta_{ml}^u|^2\} = (\tilde{b} - \tilde{a}^2) \mathbb{E}\{|\hat{\mathbf{g}}_{ml}^u{}^H \mathbf{y}_m|^2\}$; ii) Eq. (5), Eq. (45) and Eq. (47); iii) MMSE channel estimation property $\mathbf{g}_{ml}^u = \hat{\mathbf{g}}_{ml}^u + \mathbf{e}_{ml}^u$. Equality (b) follows from the results $\mathbb{E}\{|\hat{\mathbf{g}}_{ml}^u|^2\} = N_r \gamma_{ml}^u$, $\mathbb{E}\{\|\hat{\mathbf{g}}_{ml}^u\|^4\} = N_r(N_r + 1)(\gamma_{ml}^u)^2$ [28] and $\mathbb{E}\{\|\mathbf{e}_{ml}^u\|^2\} = (\beta_{ml}^u - \gamma_{ml}^u)$. The result in (15) follows from the following expression

$$S_l^u = \tau_f \log_2 \left(1 + \frac{\mathbb{E}\{|\text{DS}_l^u|^2\}}{\mathbb{E}\{|\text{BU}_l^u|^2\} + \mathbb{E}\{|\text{MUI}_l^u|^2\} + \mathbb{E}\{|\text{RI}_l^u|^2\} + \mathbb{E}\{|\text{TQD}_l^u|^2\} + \mathbb{E}\{|\text{N}_l^u|^2\}} \right).$$

We now derive the achievable SE expression for the k th downlink UE in (14). From Section II-B, we know that $\mathbf{g}_{mk}^d = \hat{\mathbf{g}}_{mk}^d + \mathbf{e}_{mk}^d$, where $\hat{\mathbf{g}}_{mk}^d$ and \mathbf{e}_{mk}^d are independent and $\mathbb{E}\{\|\hat{\mathbf{g}}_{mk}^d\|^2\} = N_t \gamma_{mk}^d$. We can express the desired signal for the k th downlink UE as

$$\mathbb{E}\{|\text{DS}_k^d|^2\} = \tilde{a}^2 \rho_d \mathbb{E} \left\{ \left| \sum_{m \in \mathcal{M}_k^d} \sqrt{\eta_{mk}} \mathbb{E}\{(\hat{\mathbf{g}}_{mk}^d)^T (\hat{\mathbf{g}}_{mk}^d)^*\} s_k^d \right|^2 \right\} = \tilde{a}^2 N_t^2 \rho_d \left(\sum_{m \in \mathcal{M}_k^d} \sqrt{\eta_{mk}} \gamma_{mk}^d \right)^2. \quad (49)$$

We now calculate the beamforming uncertainty for the k th downlink UE as

$$\begin{aligned} \mathbb{E}\{|\text{BU}_k^d|^2\} &= \tilde{a}^2 \rho_d \sum_{m \in \mathcal{M}_k^d} \mathbb{E}\{|\sqrt{\eta_{mk}} ((\mathbf{g}_{mk}^d)^T (\hat{\mathbf{g}}_{mk}^d)^* - \mathbb{E}\{(\mathbf{g}_{mk}^d)^T (\hat{\mathbf{g}}_{mk}^d)^*\})|^2\} \\ &\stackrel{(a)}{=} \tilde{a}^2 \rho_d \sum_{m \in \mathcal{M}_k^d} \eta_{mk} (N_t(N_t + 1)(\gamma_{mk}^d)^2 + N_t \gamma_{mk}^d (\beta_{mk}^d - \gamma_{mk}^d) - N_t^2 (\gamma_{mk}^d)^2) = \tilde{a}^2 N_t \rho_d \sum_{m \in \mathcal{M}_k^d} \eta_{mk} \beta_{mk}^d \gamma_{mk}^d. \end{aligned} \quad (50)$$

Equality (a) is obtained by i) using $\mathbb{E}\{|s_k^d|^2\} = 1$; ii) substituting $\mathbf{g}_{mk}^d = \hat{\mathbf{g}}_{mk}^d + \mathbf{e}_{mk}^d$; iii) using the fact that $\hat{\mathbf{g}}_{mk}^d$ are zero-mean and uncorrelated; and iv) using the results $\mathbb{E}\{\|\hat{\mathbf{g}}_{mk}^d\|^4\} = N_t(N_t + 1)(\gamma_{mk}^d)^2$ [28] and $\mathbb{E}\{\|\mathbf{e}_{mk}^d\|^2\} = (\beta_{mk}^d - \gamma_{mk}^d)$.

We now simplify the multi-UE interference for the k th downlink UE as

$$\mathbb{E}\{|\text{MUI}_k^d|^2\} = \tilde{a}^2 \rho_d \sum_{m=1}^M \sum_{q \in \kappa_{dm} \setminus k} \eta_{mq} \mathbb{E}\{|\mathbf{g}_{mk}^d{}^T (\hat{\mathbf{g}}_{mq}^d)^*|^2\} \stackrel{(a)}{=} \tilde{a}^2 N_t \rho_d \sum_{m=1}^M \sum_{q \in \kappa_{dm} \setminus k} \beta_{mk}^d \eta_{mq} \gamma_{mq}^d. \quad (51)$$

Equality (a) is because: i) $\mathbb{E}\{|s_q^d|^2\} = 1$; ii) $\hat{\mathbf{g}}_{mq}^d$ and \mathbf{g}_{mk}^d are mutually independent; and

$$\text{iii) } \mathbb{E}\{|\mathbf{g}_{mk}^d{}^T (\hat{\mathbf{g}}_{mq}^d)^*|^2\} = \mathbb{E}\{(\hat{\mathbf{g}}_{mq}^d)^T \mathbb{E}\{\mathbf{g}_{mk}^d (\mathbf{g}_{mk}^d)^T\} (\hat{\mathbf{g}}_{mq}^d)^*\} = \beta_{mk}^d \mathbb{E}\{(\hat{\mathbf{g}}_{mq}^d)^T \mathbf{I}_{N_t} (\hat{\mathbf{g}}_{mq}^d)^*\} = N_t \beta_{mk}^d \gamma_{mq}^d.$$

We now calculate the uplink downlink interference for the k th downlink UE as follows

$$\mathbb{E}\{|\text{UDI}_k^d|^2\} = \rho_u \sum_{l=1}^{K_u} \mathbb{E}\{|h_{kl}|^2\} \theta_l \stackrel{(a)}{=} \rho_u \sum_{l=1}^{K_u} \tilde{\beta}_{kl} \theta_l. \quad (52)$$

Equality (a) follows from i) $\mathbb{E}\{|h_{kl}|^2\} = \tilde{\beta}_{kl} \mathbb{E}\{|\tilde{h}_{kl}|^2\} = \tilde{\beta}_{kl}$; ii) $\mathbb{E}\{|s_l^u|^2\} = 1$. We express the total quantization distortion for the k th downlink UE as

$$\mathbb{E}\{|\text{TQD}_k^d|^2\} \approx \rho_d \sum_{m=1}^M \sum_{q \in \kappa_{dm}} \mathbb{E}\{|\mathbf{g}_{mk}^d{}^T (\hat{\mathbf{g}}_{mq}^d)^* \varsigma_{mq}^d|^2\} \stackrel{(a)}{=} (\tilde{b} - \tilde{a}^2) N_t \rho_d \sum_{m=1}^M \sum_{q \in \kappa_{dm}} \beta_{mk}^d \eta_{mq} \gamma_{mq}^d. \quad (53)$$

Equality (a) is because: i) $\mathbb{E}\{|\varsigma_{mq}^d|^2\} = (\tilde{b} - \tilde{a}^2) \eta_{mq}$; ii) quantization distortion ς_{mq}^d is independent of the wireless channels \mathbf{g}_{mk}^d and $\hat{\mathbf{g}}_{mq}^d$; and iii) of the following result:

$$\begin{aligned} \mathbb{E}\{|\mathbf{g}_{mk}^d{}^T (\hat{\mathbf{g}}_{mq}^d)^* \varsigma_{mq}^d|^2\} &= \mathbb{E}\{|\mathbf{g}_{mk}^d{}^T (\hat{\mathbf{g}}_{mq}^d)^*|^2\} \mathbb{E}\{|\varsigma_{mq}^d|^2\} = (\tilde{b} - \tilde{a}^2) \eta_{mq} \mathbb{E}_{\hat{\mathbf{g}}_{mq}^d} \{(\hat{\mathbf{g}}_{mq}^d)^T \beta_{mk}^d \mathbf{I}_{N_t} (\hat{\mathbf{g}}_{mq}^d)^*\} \\ &= (\tilde{b} - \tilde{a}^2) \eta_{mq} \beta_{mk}^d \mathbb{E}_{\hat{\mathbf{g}}_{mq}^d} \{(\hat{\mathbf{g}}_{mq}^d)^T (\hat{\mathbf{g}}_{mq}^d)^*\} = (\tilde{b} - \tilde{a}^2) N_t \beta_{mk}^d \eta_{mq} \gamma_{mq}^d. \end{aligned}$$

The result in (14) follows from the following expression for the achievable SE lower bound:

$$S_k^d = \tau_f \log_2 \left(1 + \frac{\mathbb{E}\{|\text{DS}_k^d|^2\}}{\mathbb{E}\{|\text{BU}_k^d|^2\} + \mathbb{E}\{|\text{MUI}_k^d|^2\} + \mathbb{E}\{|\text{UDI}_k^d|^2\} + \mathbb{E}\{|\text{TQD}_k^d|^2\} + \mathbb{E}\{|w_k^d|^2\}} \right).$$

REFERENCES

- [1] T. Marzetta, “Noncooperative cellular wireless with unlimited numbers of base station antennas,” *IEEE Trans. Wireless Commun.*, vol. 9, no. 11, pp. 3590–3600, Nov. 2010.
- [2] H. Q. Ngo, A. Ashikhmin, H. Yang, E. G. Larsson, and T. L. Marzetta, “Cell-free massive MIMO versus small cells,” *IEEE Trans. Wireless Commun.*, vol. 16, no. 3, pp. 1834 – 1850, Mar. 2017.
- [3] S. Buzzi and C. D’Andrea, “Cell-free massive MIMO: User-centric approach,” *IEEE Wireless Commun. Lett.*, vol. 6, no. 6, pp. 706 – 709, Aug. 2017.
- [4] T. Riihonen, S. Werner, and R. Wichman, “Mitigation of loopback self-interference in full-duplex MIMO relays,” *IEEE Trans. Signal Process.*, vol. 59, no. 12, pp. 5983–5993, 2011.
- [5] T. T. Vu, D. T. Ngo, H. Q. Ngo, and T. Le-Ngoc, “Full duplex cell-free massive MIMO,” in *2019 IEEE Int. Conf. on Commun. (ICC’19)*, 2019.
- [6] D. Wang, M. Wang, P. Zhu, J. Li, J. Wang, and X. You, “Performance of network-assisted full-duplex for cell-free massive MIMO,” *IEEE Trans. Commun.*, vol. 68, no. 3, pp. 1464–1478, 2020.
- [7] H. V. Nguyen, V. Nguyen, O. A. Dobre, S. K. Sharma, S. Chatzinotas, B. Ottersten, and O. Shin, “A novel heap-based pilot assignment for full duplex cell-free massive MIMO with zero-forcing,” in *2020 IEEE Int. Conf. on Commun. (ICC’20)*, 2020, pp. 1–6.
- [8] M. Bashar, K. Cumanan, A. G. Burr, H. Q. Ngo, M. Debbah, and P. Xiao, “Max–min rate of cell-free massive MIMO uplink with optimal uniform quantization,” *IEEE Trans. Commun.*, vol. 67, no. 10, pp. 6796 – 6815, Oct. 2019.

- [9] G. Femenias and F. Riera-Palou, "Cell-free millimeter-wave massive MIMO systems with limited fronthaul capacity," *IEEE Access*, vol. 7, pp. 44 596 – 44 612, Apr. 2019.
- [10] H. Masoumi and M. J. Emadi, "Performance analysis of cell-free massive MIMO system with limited fronthaul capacity and hardware impairments," *IEEE Trans. Wireless Commun.*, vol. 19, no. 2, pp. 1038–1053, 2020.
- [11] H. Ngo, L. Tran, T. Q. Duong, M. Matthaiou, and E. G. Larsson, "On the total energy efficiency of cell-free massive MIMO," *IEEE Trans. on Green Commun. and Networking*, vol. 2, no. 1, pp. 25 – 39, Mar. 2018.
- [12] M. Bashar, K. Cumanan, A. G. Burr, H. Q. Ngo, E. G. Larsson, and P. Xiao, "Energy efficiency of the cell-free massive MIMO uplink with optimal uniform quantization," *IEEE Trans. on Green Commun. and Networking(Early Access)*, 2019.
- [13] M. Alonzo, S. Buzzi, A. Zappone, and C. D'Elia, "Energy-efficient power control in cell-free and user-centric massive MIMO at millimeter wave," *IEEE Trans. on Green Commun. and Networking*, pp. 651 – 663, Sept. 2019.
- [14] H. V. Nguyen, V. Nguyen, O. A. Dobre, S. K. Sharma, S. Chatzinotas, B. Ottersten, and O. Shin, "On the spectral and energy efficiencies of full-duplex cell-free massive MIMO," *IEEE J. Sel. Areas Commun.*, Jun. 2020, Early Access.
- [15] A. Zappone and E. Jorswieck, *Energy Efficiency in Wireless Networks via Fractional Programming Theory*. Now Foundations and Trends, Delft, Netherlands, 2015.
- [16] C. N. Efrem and A. D. Panagopoulos, "A framework for weighted-sum energy efficiency maximization in wireless networks," *IEEE Wireless Commun. Lett.*, vol. 8, no. 1, pp. 153–156, 2019.
- [17] E. Sharma, D. N. Amudala, and R. Budhiraja, "Energy efficiency optimization of massive MIMO FD relay with quadratic transform," *IEEE Trans. Wireless Commun.*, vol. 19, no. 2, pp. 1429–1448, 2020.
- [18] C. Jeon, K. Li, J. R. Cavallaro, and C. Studer, "Decentralized equalization with feedforward architectures for massive MU-MIMO," *IEEE Trans. Signal Process.*, vol. 67, no. 17, pp. 4418–4432, 2019.
- [19] J. Rodríguez Sánchez, F. Rusek, O. Edfors, M. Sarajlić, and L. Liu, "Decentralized massive MIMO processing exploring daisy-chain architecture and recursive algorithms," *IEEE Trans. Signal Process.*, vol. 68, pp. 687–700, 2020.
- [20] Z. Zhou, J. Feng, Z. Chang, and X. Shen, "Energy-efficient edge computing service provisioning for vehicular networks: A consensus ADMM approach," *IEEE Trans. Veh. Technol.*, vol. 68, no. 5, pp. 5087 – 5099, May 2019.
- [21] E. Sharma, S. S. Chauhan, and R. Budhiraja, "Decentralized WSEE optimization for massive MIMO two-way half-duplex AF relaying," *IEEE Wireless Commun. Lett.*, vol. 19, no. 2, pp. 1397 – 1414, Feb. 2020.
- [22] S. Boyd and L. Vandenberghe, *Convex optimization*. Cambridge university press, 2004.
- [23] S. Boyd, N. Parikh, E. Chu, B. Peleato, and J. Eckstein, "Distributed optimization and statistical learning via the alternating direction method of multipliers," *Foundations and Trends in Machine Learning*, vol. 3, no. 1, pp. 1 – 122, 2010.
- [24] A. Beck, A. Ben-Tal, and L. Tetruashvili, "A sequential parametric convex approximation method with applications to nonconvex truss topology design problems," *Journal of Global Optimization*, vol. 47, no. 1, pp. 29–51, May 2010.
- [25] B. He, H. Yang, and S. Wang, "Alternating direction method with selfadaptive penalty parameters for monotone variational inequalities," *Journal of Optimization Theory and Applications*, vol. 106, no. 2, p. 337–356, Aug. 2000.
- [26] A. Ben-Tal and A. Nemirovski, *Lectures on Modern Convex Optimization: Analysis, Algorithms, and Engineering Applications*. Society for Industrial and Applied Mathematics, Philadelphia, USA, 2001.
- [27] H. Q. Ngo, A. Ashikhmin, H. Yang, E. G. Larsson, and T. L. Marzetta, "Relationship between two distortion measures for memoryless nonlinear systems," *IEEE Trans. Wireless Commun.*, vol. 17, no. 11, pp. 917 – 920, Nov. 2010.
- [28] A. M. Tulino and S. Verdu, "Random matrix theory and wireless communications," *Foundations and Trends in Communications and Information Theory*, vol. 1, no. 1, pp. 1 – 182, 2004.